VCP/p97 extracts DNA polymerase α/Primase from chromatin to limit the activation of the replication stress response

Sara Rodríguez-Acebes[1#], Rodrigo Martín-Rufo[2#], Alejandro Fernández-Llorente[2], Guillermo de la Vega-Barranco[2], Pilar Oroz[2], Elena Martín-Doncel[3], Luis Ignacio Toledo[3], Juan Méndez[1], Emilio Lecona[2]

1 DNA Replication Group, Spanish National Cancer Research Centre (CNIO), Madrid 28029, Spain
2 Chromatin, Cancer and the Ubiquitin System lab, Centre for Molecular Biology Severo Ochoa (CBMSO, CSIC-UAM), Department of Genome Dynamics and Function, Madrid 28049, Spain
3 Center for Chromosome Stability, Institute for Cellular and Molecular Medicine, Faculty of Health and Medical Sciences, University of Copenhagen, Copenhagen 2200, Denmark

# equally contributed

Correspondence: Emilio Lecona (elecona@cbm.csic.es),

ABSTRACT

The replication stress response is an essential pathway that deals with the lesions that halt the progression of DNA replication forks even during an unperturbed S phase. Basal activation of the ATR and CHK1 kinases prevents the premature firing of origins of replication during S phase, avoiding the activation of an excessive number of replication forks and the appearance of genomic instability. However, the mechanisms that regulate ATR activation in the unperturbed S phase have not been fully determined. Here we present evidence showing that the AAA ATPase VCP/p97 regulates the presence of the DNA polymerase α/Primase complex (POLA/PRIM) on chromatin after origin firing, thus limiting the generation of primed DNA structures that mediate the activation of ATR by TOPBP1. As a consequence, inhibiting VCP/p97 activates ATR and CHK1 leading to cell cycle arrest in G2/M. We propose that the loading of POLA/PRIM after origin firing drives the basal activation of ATR during an unperturbed S phase and VCP/p97 regulates this activation through the extraction of POLA/PRIM from chromatin.

INTRODUCTION

DNA replication is the ordered sequence of events that leads to the faithful duplication of the genetic material in a cell while preventing the appearance of mutations and genomic alterations that fuel genomic instability. However, in each S phase the advance of replication forks is challenged by the presence of alterations in the DNA or difficult to replicate regions that lead to the stalling of DNA polymerases, the accumulation of single stranded DNA (ssDNA), the activation of the replication stress response (RSR) and the replication-coupled DNA repair mechanisms[1,2,3]. The RSR is mainly driven by the kinase ATR and its downstream effector, the CHK1 kinase. Together, these kinases stabilize stalled DNA replication forks, inhibit new origin firing and activate the G2/M checkpoint to prevent the progression into mitosis in the presence of unreplicated DNA[4]. Both ATR and CHK1 are essential, reflecting the fundamental role of the RSR in every round of DNA replication, even in the absence of exogenous DNA damage[5]. In this sense, it has been shown that ATR activity fluctuates during S phase to control the rate of DNA replication and that the basal activation of ATR monitors the accumulation of RPA in replication forks[6,7].

DNA synthesis is preceded by the formation of pre-replicative complexes at origins in G1. Origin firing sets the start of S phase through the phosphorylation and activation of the CMG helicase leading to the opening of the DNA double helix required for the loading of the replication machinery[8]. During DNA replication elongation the CMG helicase advances through chromatin opening the DNA while the replicative DNA polymerases synthesize new DNA[9,10]. First, the DNA polymerase α/Primase complex (POLA/PRIM) generates RNA-DNA primers that are the substrate for DNA polymerase δ. In the leading strand, DNA polymerase δ is quickly replaced by DNA polymerase ε that travels with the CMG helicase to continuously synthesize this strand. In contrast, the lagging strand requires multiple priming events by POLA/PRIM to generate the discontinuous Okazaki fragments that are synthesized by DNA polymerase δ.

Ubiquitylation and SUMOylation of DNA replication factors influences every step in DNA replication and repair, constituting one of the key mechanisms to maintain genomic stability[11–13]. The proteomic analysis of nascent chromatin revealed the presence of a SUMO-rich environment associated to DNA replication forks[14,15].

We have shown that the ubiquitin/SUMO landscape in chromatin is maintained by a coordinated action of the deubiquitinase USP7 and the AAA ATPase VCP/p97[16,17]. While USP7 removes ubiquitin from SUMOylated proteins in the replication forks, VCP/p97 extracts SUMOylated and ubiquitylated proteins from chromatin during DNA replication. VCP/p97 is a molecular machine that assembles as a ring-shaped homohexameric complex with a central pore where the ATPase domains are located[18,19]. VCP/p97 extracts proteins from chromatin when they are no longer needed to allow their degradation or recycling. During DNA replication, this protein is responsible for the extraction and degradation of CDT1 to prevent re-replication in S phase[20,21], and for the removal of the replisome upon MCM7 ubiquitylation during DNA replication termination or in response to DNA damage[12,22,23,24]. A wide variety of cofactors dock on top of the VCP/p97 ring and mediate the binding of specific substrates through the recognition of ubiquitylated and SUMOylated proteins[25]. Recent biochemical data show that, once the ubiquitylated substrate has been positioned by the cofactors on top of VCP/p97, a distal ubiquitin molecule in the chain is unfolded to promote the subsequent extrusion of the protein through the central pore of the complex[26–28].

Here we dissect the functions of VCP/p97 during the initiation and elongation phases of DNA replication. We identify POLA/PRIM as a target of VCP/p97 and we show that it limits the concentration of POLA/PRIM complexes on chromatin upon origin firing. The accumulation of POLA/PRIM induced by VCP/p97 inhibition raises the basal level of activation of the RSR in an unperturbed S phase. Thus, VCP/p97 limits the activation of the RSR through the extraction of POLA/PRIM from chromatin. Our results provide a model to explain how cells control the number of active DNA replication forks by sensing origin firing through the activation of the RSR induced by POLA/PRIM.

RESULTS

VCP/p97 controls DNA replication

To analyze the functions of VCP/p97 during DNA replication we synchronized HCT116 colon adenocarcinoma cells in G1/S phase using a single thymidine block. After the cells progressed into S phase the action of VCP/p97 was blocked using the specific allosteric inhibitor NMS873 (from here on VCPi)[29]. As we have reported before[17], the inhibition of VCP/p97 impairs DNA synthesis in a time- and dose-dependent manner as shown by the decrease in EdU incorporation measured by flow cytometry (Figure 1A-B). To characterize this function in detail, we investigated the effects of VCP/p97 inhibition on the dynamics of DNA replication using stretched DNA fibers. In these experiments synchronized HCT116 cells were treated with VCP/p97 inhibitor and then incubated sequentially with chlorodeoxyuridine (CldU) and iododeoxyuridine (IdU) (both in the presence of VCP/p97 inhibitor) to measure fork rate (Figure 1C, FR) and origin firing (Figure 1C, 1st label origins). Blocking the activity of VCP/p97 led to a slight but consistent decrease in fork speed (Figure 1D) along with a strong inhibition of origin firing (Figure 1E). The analysis of termination events did not reveal any differences (Figure S1A), as anticipated because VCP/p97 is required for the disassembly of the replication machinery that only happens after the actual termination of DNA replication. We measured the effect of VCP/p97 on fork symmetry using a modified version of the stretched DNA fiber assay to evaluate: the asymmetry of ongoing forks through the ratio of both labels (Figure 1F, CldU/IdU); origin asymmetry through the ratio between the two tracks for the second label in a fiber originating from a single origin (Figure 1F, long/short)[30]. The inhibition of VCP/p97 led to an increase in the CldU/IdU ratio (Figure 1G), indicative of a high frequency of stalled forks rather than reduced fork speed/impaired replication processivity[30]. VCPi also increased the degree of asymmetry between the two forks emanating from an origin (Figure 1H and S1B-C) and the percentage of “asymmetric origins” was increased 4-fold (Figure S1D). We wondered if the induction of fork and origin asymmetry could be due to an effect of VCP/p97 on the RSR. Synchronized HCT116 cells were treated with hydroxyurea (HU), an agent that depletes the pool of dNTPs through the inhibition of the ribonucleotide reductase leading to fork stalling and the activation of the RSR. As expected, the treatment with HU increased the phosphorylation of CHK1

by ATR (CHK1-S345P) and the levels of γH2AX (Figure 1I, lanes 1-4). In addition, HU increased the phosphorylation of RPA2 by ATM (RPA2-S4/8P) suggesting that forks have collapsed and generated DNA double strand breaks (DSB) (Figure 1I, lanes 1-4). Inhibiting VCP/p97 did not change the activation of the RSR by HU, showing a similar pattern of CHK1 phosphorylation and γH2AX accumulation (Figure 1I, compare lanes 2-4 with 5-7). We observed a reduction in the phosphorylation of RPA2 in the presence of VCPi after HU treatment (Figure 1I, compare lanes 4 and 7). This effect is most likely due to the lower fork speed caused by VCP/p97 inhibition that could limit the amount of ssDNA generated in the presence of HU. Of note, the inhibition of VCP/p97 without HU led to a slight but consistent increase in the phosphorylation of CHK1 without inducing changes in the phosphorylation of RPA2 (Figure 1I, lanes 8-10). These data suggest that the changes in DNA replication dynamics induced by VCP/p97 inhibition activate ATR without inducing fork collapse or DNA damage.

A dual function of VCP/p97 in origin firing and DNA replication fork progression

The changes in origin firing and fork speed are usually inversely correlated to ensure the complete copy of DNA in S phase[31]. Interestingly, VCP/p97 inhibition induced a strong block in origin firing along with a small decrease in fork speed, suggesting that VCP/p97 is necessary for both processes. To confirm if VCP/p97 plays a role during elongation, nucleosides were added to speed up DNA replication forks. As previously described[32,33], nucleoside supplementation increased fork speed with a concomitant reduction in new origin firing (Figure 2A-B). The fact that VCPi prevented the increase in fork speed induced by nucleosides without changing origin firing inhibition (Figure 2A-B), supports a direct role for VCP/p97 in sustaining elongation. In addition, inhibition of CDC7 (CDC7i), the kinase responsible for the activation of the CMG helicase[34] led to a strong decrease in origin firing and a concomitant increase in fork rate (Figure 2C-D). Similar to what we observed with nucleoside supplementation, the inhibition of VCP/p97 blocked the increase in fork rate induced by CDC7i without further inhibiting origin firing (Figure 2C-D). Combined, these experiments show that VCP/p97 is required for elongation and suggest that it might not be necessary for the activation of the signaling pathway that sets origin firing itself. In

agreement with this notion, VCPi did not significantly affect the phosphorylation of MCM2 (Figure S2A).

We hypothesized that the apparent decrease in origin firing observed in DNA fibers after VCP/p97 inhibition could reflect a blockage of the steps in DNA replication that immediately follow origin activation. Thus, we blocked DNA replication right after origin firing by inhibiting DNA polymerase α with adarotene/ST1926 (POLAi)[35]. The formation of new forks is strongly reduced when POLA is inhibited, leading to an increase in the speed of ongoing replication forks (Figure 2E-F). Concomitant inhibition of POLA and VCP/p97 did not have any further effect on fork rate or DNA replication initiation, indicating that both proteins operate in the same pathway (Figure 2E-F). The fact that VCPi cannot prevent the increase in fork speed elicited by POLA1i while it blocks the effect of CDC7i suggests that POLA/PRIM is also relevant for the effect of VCP/p97 during DNA replication elongation.

POLA inhibition has been reported to uncouple the progression of the leading and the lagging strands[36]. In line with these results, fork asymmetry was increased when POLA was inhibited and this increase was similar to the effect of VCP/p97 inhibition (Figure 2G-H and S2B-F). The simultaneous block of POLA and VCP/p97 did not elicit any further increase in asymmetry measured through the ratio CldU/IdU in a single track, the ratio of long/short fork length from a single origin or the percentage of asymmetric origins (Figure 2G-H and S2B-F), again indicating the epistatic relation of VCP/p97 and POLA in the control of DNA replication. Supporting this idea, both POLA and VCP/p97 can directly limit accelerated fork progression induced by CDC7i (Figure 2C and 2I) without further reducing origin firing (Figure 2D and 2J).

To further characterize the functional cooperation between VCP/p97 and POLA during DNA replication, we analyzed the activation of the RSR when both proteins are blocked. As reported[36], POLA inhibition led to a dose-dependent activation of ATR leading to CHK1 phosphorylation (Figure 2K, lanes 1-5). At higher doses, POLAi generated DSB and DNA damage measured by the increase in γH2AX, consistent with replication catastrophe[36] (Figure 2K, lanes 1-5). Inhibiting VCP/p97 in the presence of POLA inhibitors did not change the induction of damage but led to stronger phosphorylation of CHK1 at all the concentrations of POLAi (Figure 2K, compare lanes 1-5 and 6-10). None of the treatments changed

the levels of VCP/p97 or POLA1, and the inhibition of VCP/p97 only led to a slight accumulation of ubiquitylated proteins in these conditions (Figure S2G). These data indicate that VCPi does not prevent RPA exhaustion and replication catastrophe caused by POLAi. Instead, POLA cooperates with VCP/p97 to regulate ATR activity and CHK1 phosphorylation during unperturbed DNA replication.

VCP/p97 extracts POLA/PRIM from chromatin

Work by the Cimprich lab proved that the accumulation of DNA primers generated by POLA/PRIM promotes TOPBP1 loading on chromatin and stimulates the activation of ATR[37]. Since the inhibition of VCP/p97 and POLA synergize in the activation of CHK1, we tested if VCP/p97 could directly extract POLA/PRIM to limit the activation of the RSR. First, we carried out pull-down experiments using cross-linked samples since the interaction of VCP/p97 with its substrates and adaptors is very labile[38]. The immunoprecipitation (IP) of VCP/p97 from cross-linked chromatin extracts recovered POLA1 in control conditions, as well as after the treatment with VCPi and POLAi (Figure S3A). This interaction was confirmed with reciprocal pull-down experiments with antibodies against VCP/p97 and PRIM2 (PRIM2 was chosen because the IP of other components of the POLA/PRIM complex was either ineffective or disrupted the complex). PRIM2 IP recovered POLA1 in control conditions as well as after treatment with VCPi or POLAi (Figure 3A), indicating that the whole POLA/PRIM complex was pulled-down. In addition, PRIM2 immunoprecipitate contained VCP/p97 and the interaction was increased after VCPi treatment (Figure 3A), as expected because the binding of VCP/p97 to its substrates is stabilized by substrate-trapping[39,40]. Conversely, VCP/p97 pull-down recovered POLA1, confirming the interaction (Figure 3A). Interestingly, VCP/p97 pulled-down a specific band in POLA1 that could be a either a specific isoform of the protein, or a ubiquitylated/SUMOylated form of one of the isoforms. We confirmed that this band is POLA1 since it is pulled-down with a specific antibody (Figure S3B). PRIM2 was not consistently pulled-down by VCP/p97, probably indicating that the interaction is established through POLA1 or that the pull-down of VCP/p97 disrupts the interaction between the polymerase and the primase complexes. As a negative control, none of the pull-downs contained RPA2 (Figure 3A).

Having established the binding of POLA/PRIM by VCP/p97, we analyzed if VCPi would lead to the accumulation of POLA/PRIM on chromatin. Both POLA1 and PRIM2 slightly accumulated on chromatin when VCP/p97 was inhibited during S phase (Figure 3B). Importantly, the total levels of POLA1 or VCP/p97 are not altered by VCP/p97 inhibition as observed in whole cell extracts (Figure S2G). As expected, VCPi led to the accumulation of VCP/p97 on chromatin too, while the levels of PCNA and histone H2A remained unaltered (Figure 3B). These data suggested that VCP/p97 extracts POLA/PRIM from chromatin during DNA replication.

In vitro replication experiments using *Xenopus* egg extracts have shown that POLA accumulation on chromatin and the subsequent activation of ATR requires origin firing but can also be stimulated by the synthesis of new primers ahead of the stalled fork[37,41,42]. Thus, we explored if the activation of CHK1 upon VCP/p97 inhibition was related to repriming ahead of stalled forks and/or to priming actions upon new origin firing. The primase/polymerase PRIMPOL mediates repriming in the presence of DNA damage[43,44]. Genetic depletion of PRIMPOL[45] did not change the effect of VCPi on DNA replication (Figure S3C), arguing against an effect of VCP/p97 inhibition on PRIMPOL-mediated repriming. In contrast, blocking origin firing through the inhibition of CDC7 led to a decrease in the accumulation of VCP and PRIM2 on chromatin observed after treatment with VCPi (Figure 3C, lane 2 vs 7); this effect is stronger when CDC7 is inhibited in cells treated with a combination of VCPi and POLAi (Figure 3C, lane 6 vs 8). This suggests that the extraction of POLA/PRIM by VCP/p97 from chromatin happens after origins firing in agreement with the results from the DNA fiber assays. Interestingly, the reduction in the amount of POLA/PRIM on chromatin was mirrored by a decrease in the phosphorylation of CHK1 in the soluble nuclear fraction (Figure 3C, lane 2 versus 7, and lane 6 versus 8). Further, the inhibition of CDC7 reduced the accumulation of RPA2 on chromatin induced by POLAi (Figure 3C, lanes 3 versus 5 and 6 versus 8). As a control the levels of histone H2A and USP7 were not altered (Figure 3C). The analysis of the cell cycle showed that CDC7i led to a slight rescue in EdU compared to the combined treatment of VCPi and POLAi (Figure S3D, lower row, compare first and last samples).

These results are in line with a recent report that shows that CDC7 activity is required for CHK1 activation during unperturbed S phase[46] and suggest that the accumulation of POLA/PRIM on chromatin after origin firing leads to the activation of ATR. ATR activation is a two-step process mediated by the recruitment of the ATR-ATRIP complex to ssDNA by RPA and its activation through specific domains in TOPBP1 or ETAA1. While TOPBP1 is recruited to ssDNA/dsDNA junctions and requires the presence of primed DNA, ETAA1 directly binds to the RPA complex and its action is linked to the accumulation of ssDNA. Interestingly, the phosphorylation of CHK1 caused by VCPi was dependent on the presence of TOPBP1 (Figure 3D, siTOPBP1), while the depletion of ETAA1 using a previously validated siRNA[36] did not have any effect on the activation of ATR by VCP/p97 inhibition (Figure 3D, siETAA1 and Figure S3E). We conclude that VCP/p97 controls the accumulation of POLA/PRIM on chromatin and can limit the generation of primed DNA that serves as a substrate for TOPBP1 mediated ATR activation.

POLA/PRIM depletion prevents ATR activation by VCPi

If our model is correct, the activation of ATR by VCPi should depend on the presence of POLA/PRIM on chromatin. To test whether this is the case we depleted the four components of the POLA/PRIM complex using previously validated siRNA pools[36]. Depletion of POLA1 or POLA2, but not PRIM1 or PRIM2, led to a decrease in the levels of POLA1; conversely, depletion of PRIM1 and PRIM2 led to reduced levels of these proteins without affecting POLA1 (Figure S4A-B). CHK1 phosphorylation was increased upon VCPi treatment in cells transfected with a non-specific siRNA and this effect was much attenuated when the levels of POLA or PRIM complexes were reduced (Figure 4A-B). Thus, a reduction in the levels of the POLA/PRIM complex prevented the increase in CHK1 phosphorylation induced by the inhibition of VCP/p97. This effect contrasts with the synergistic activation of ATR observed after concomitant inhibition of POLA and VCP/p97 that leads to an increased retention of POLA/PRIM on chromatin (Figure 2K). This difference indicates that ATR activation induced by VCPi requires the retention of POLA/PRIM on chromatin (Figure 3C-D) driving the generation of primed DNA and the recruitment of TOPBP1.

The depletion of POLA1 increased fork speed and reduced origin firing to a similar extent as inhibiting POLA (Figure 4C-D). The incubation with VCPi did not revert the increase in fork rate or induce a further decrease in origin firing (Figure 4C-D), similar to what we observed with the POLAi and VCPi combination (Figure 2E-F). Depletion of PRIM2 led to a similar effect although it did not inhibit origin firing (Figure 4C-D). In contrast to the acute inhibition of POLA1, the depletion of POLA1 or PRIM2 did not lead to an increase in fork asymmetry (Figure S4C-J). However, while VCPi increased fork asymmetry in control cells, the inhibition of VCP/p97 in POLA1 or PRIM2 depleted cells did not change fork or origin asymmetry (Figure S4C-I). Thus, depleting POLA/PRIM has similar effects to POLAi in DNA replication dynamics, yet it prevents the increase in activation of CHK1 induced by VCPi. When the levels of POLA/PRIM are limiting, blocking VCP/p97 cannot elicit its accumulation and the activation of CHK1 is not observed. In this sense, the concentration of adarotene/ST1926 used in our experiments are unlikely to completely inhibit POLA1, since the total blockage of the primer extension activity of POLA1 requires a 5-10 times higher concentration than the one used in our experiments[35]. An incomplete inactivation of POLA1 would lead to the accumulation of unfinished, not elongated primers which would activate ATR via TOPBP1. The inhibition of VCP/p97 could lead to a longer half-life of these primers by preventing the extraction of POLA/PRIM and explain the synergistic activation of CHK1 in the presence of POLAi. In contrast, the depletion of the POLA/PRIM complex would prevent the accumulation of these primers and the inhibition of VCP/p97 would have no effect on CHK1 activation under these conditions.

VCP/p97 prevents G2/M checkpoint activation during unperturbed DNA replication

Based on our results we propose a model where VCP/p97 limits the amount of POLA/PRIM on chromatin after origins of replication are fired (Figure 5A). During unperturbed DNA replication, VCP/p97 would prevent an excessive engagement of POLA/PRIM complexes and maintain the basal level of ATR activation through S phase (Figure 5A, top). The accumulation of POLA/PRIM on chromatin induced by VCP/p97 inhibition leads to TOPBP1-mediated activation of ATR and the phosphorylation of CHK1 (Figure 5A, bottom). Last, we decided to evaluate if the

activation of CHK1 by VCPi leads to a functional activation of the G2/M checkpoint. In agreement with previous results[29], the inhibition of VCP/p97 led to the arrest of the cell cycle in G2/M (Figure 5B) that has been linked to the inhibition of replisome disassembly after DNA replication termination[47]. However, our results raise the possibility that the increase in CHK1 phosphorylation induced by VCPi during the whole S phase directly activates the G2/M checkpoint. In fact, the inhibition of CHK1 allowed cells to bypass the checkpoint and progress through mitosis into G1 even in the presence of VCPi (Figure 5B). One of the main effectors of CHK1 in the G2/M checkpoint is the CDC25 family of protein phosphatases that are destabilized or sequestered by their phosphorylation by CHK1[48]. As expected, CHK1 inhibition led to a shorter G2/M phase (Figure 5B) and the induction of high levels of DNA damage as observed by the increase in γH2AX and RPA2 phosphorylation (Figure 5C). Interestingly, the arrest in G2/M induced by the inhibition of VCP/p97 (Figure 5B) was accompanied by a decrease in the levels of CDC25A (Figure 5C). The levels of CDC25A were not rescued by the concomitant inhibition of CHK1 and VCP/p97 (Figure 5C). This could be a secondary effect of the replication catastrophe induced by CHK1i that leads to the activation of ATM promoting the degradation of CDC25A. Of note, VCP/p97 inhibition reduced the DNA damage elicited by CHK1 inhibition and led to a reduction in the phosphorylation of CHK1 itself (Figure 5C). These data suggest that CHK1 phosphorylation induced by VCPi leads to the activation of the G2/M checkpoint but CDC25A stabilization is not essential for cell cycle arrest. Our data suggest that VCP/p97 prevents the activation of the G2/M checkpoint during an unperturbed S phase by limiting the activation of ATR.

DISCUSSION

The mechanisms of activation of the RSR have been mainly elucidated employing different kinds of insults that induce replication stress by uncoupling the CMG helicase and the replicative DNA polymerases, and leading to the accumulation of ssDNA[2]. However, ATR is also activated during an unperturbed S phase and is essential, even in the absence of damage, to sustain the full and accurate replication of the cellular DNA[5]. Interestingly, the subset of targets phosphorylated by ATR during S phase differs from the proteins modified by ATR in the presence of replication stress[49,50]. Initial reports showing that ATR and CHK1 inhibition accelerated DNA replication led to the suggestion that the basal activation of the RSR restricts origin firing to prevent the depletion of resources necessary during DNA replication[51,52]. Later it was shown that the activation of a limited number of ATR molecules prevents the phosphorylation of MCM4 and the GINS complex by CDC7 to inhibit new origin firing both locally and in late S phase[53,54]. Inhibiting ATR in the absence of damage increases the number of active replication forks and the rate of DNA replication at the price of decreased fork speed and an accumulation of collapsed forks[55]. Thus, the basal ATR activity limits the number of origins that are activated simultaneously, independent of the presence of replication stress, to ensure the correct progression of DNA replication. Interestingly, the basal level of ATR activity has been recently proposed to be related to the accumulation of RPA during DNA replication[7].

Our results suggest that the basal activation of ATR is driven by the loading of POLA/PRIM on chromatin after origin firing and is restricted by the extraction of this complex by VCP/p97. This model is supported by different lines of evidence. First, ATR activation by VCPi is TOPBP1 dependent, indicating that primed DNA structures are generated when VCP/p97 is blocked (Figure 3). Second, VCPi activation of CHK1 requires the presence of POLA/PRIM, supporting a role for this complex in generating the primed DNA to sustain basal ATR activation (Figure 4). Third, origin firing is required for the accumulation of PRIM2 and VCP/p97 on chromatin and for CHK1 activation induced by VCPi (Figure 3). We note that in this context, priming events were linked to POLA/PRIM and not to PRIMPOL, as genetic ablation of the latter did not the effect of VCP/p97 inhibition on cell cycle progression. In fact, our experimental conditions involve a partial inhibition of POLA/PRIM that would allow the generation of primers that mediate

ATR activation[35]. Under these conditions the leading and lagging strand synthesis are uncoupled, probably due to problems in the generation of Okazaki fragments[36]. In contrast, a higher concentration of POLA1 inhibitor affects both leading and lagging strand progression and prevents CHK1 activation[56], probably due to the absence of primed ssDNA/dsDNA structures.

Based on these data, we propose that every time DNA is opened at an origin of replication, the loading of POLA/PRIM complexes generates primed DNA structures that sustain basal activation of ATR (Figure 5A). To prevent an excessive activation of ATR, VCP/p97 extracts POLA/PRIM from chromatin. POLA/PRIM is recruited to chromatin by different mechanism: through the CST complex in telomeres and during NHEJ[57,58]; by RAD51 at stalled DNA replication forks[59]; or by AND1 to active replication forks[60]. Recently, the reconstitution of DNA replication with purified proteins *in vitro* has shown that POLA/PRIM is still recruited to active forks in the absence of AND-1[61] and it has been proposed that POLA/PRIM presents a distributive association with the replication fork[62]. This mode of association would support the idea of loading of several POLA/PRIM molecules before the two active replication forks are established. We hypothesize that the extraction of POLA/PRIM by VCP/p97 participates in the establishment of the active forks after origin firing.

CHK1 phosphorylation upon VCPi leads to the activation of the checkpoint and the arrest of the cell cycle in G2/M. Since VCP/p97 unloads the replisome upon DNA replication termination[63], it has been previously proposed that the G2/M arrest induced by VCPi is related to the accumulation of replication proteins on chromatin[47]. A recent study has shown that replisome disassembly in S phase is necessary to recycle DNA replication factors. Deleting the E3 ubiquitin ligase that marks the replisome for the extraction by VCP/p97 activates the G2/M checkpoint[47]. However, this study did not analyze if VCP/p97 inhibition itself would induce such an effect. Here we show that VCP/p97 directly restricts the activation of the RSR in the absence of replication stress. Thus, checkpoint activation by VCPi might be the consequence of enhanced basal CHK1 phosphorylation together with the accumulation of unloaded replisomes in late S phase that limit the availability of replication factors.

Beyond understanding how VCP/p97 controls the basal activation of ATR and CHK1, these results are relevant for the application of VCP/p97 inhibitors in

cancer treatment. The inhibition of VCP/p97 was initially proposed to induce cancer cell death through an increase in proteotoxic stress[64,65]. However, recent data support a more relevant role for the regulation of DNA replication and repair[22]. In fact, VCPi increases PARP1 trapping and sensitizes homologous deficient tumors to the treatment with PARP inhibitors[66]. Further, the anti-alcohol abuse drug disulfiram targets the VCP/p97 adaptor NPL4 and interferes with the RSR to prevent cancer development[67,68]. VCP/p97 inhibition also sensitizes cancer cells to the induction of DNA damage by altering DNA repair pathway choice[69–71].

In addition to the control of POLA/PRIM accumulation on chromatin after origin firing, our data puts forward a role for VCP/p97 in the control of DNA replication fork progression. VCP/p97 participates in different steps of DNA replication: it extracts CDT1 during DNA replication initiation[20,21], maintains the ubiquitin/SUMO equilibrium during the elongation phase[16,63,72], and removes the replisome from chromatin upon DNA replication termination[63,73]. We show that VCP/p97 activity is necessary to sustain a physiological fork rate in a POLA/PRIM dependent manner, and this effect could be mediated by several mechanisms. First, the removal of POLA/PRIM by VCP/p97 could facilitate the switch to DNA polymerases δ and ε to allow the progression from initiation to elongation. Second, VCP/p97 could be required to recycle other limiting replication factors, as suggested by recent work in mammalian cells[47]. Last, VCPi could lead to the uncoupling of the leading and lagging strands similar to the effects of POLA inhibition. Further experiments will be required to fully understand how VCP/p97 determines DNA replication dynamics and to identify what cofactors participate in each of these processes.

In summary, here we have gained insight into the functions of VCP/p97 during an unperturbed S phase. We have shown that basal ATR activation, essential for the progression of S phase, is triggered by POLA/PRIM loading upon origin firing and VCP/p97 limits the activation of the RSR to prevent the activation of the G2/M cell cycle checkpoint. In this sense, we had previously hypothesized that origin firing is the signal that locally prevents the firing of back-up origins[74]. This model implies that the number of active replication forks in the cell is sensed by the cumulative activation of ATR and CHK1 induced by origin firing. This mechanism

explains how cells count the number of active DNA replication forks preventing excessive origin firing that fosters replication stress and genomic instability.

MATERIALS AND METHODS

Cell lines, extract preparation, transfections and treatments.

HCT116 wild-type and PRIMPOL knockout, and U2OS cells were grown in DMEM with 10% FBS, penicillin (100 IU/ml), streptomycin (100 mg/ml) and glutamine (300 mg/ml). For passaging, cells were washed once with warm PBS and trypsinized with Trypsin-EDTA. Trypsin was inactivated by the addition of fresh media and the cell suspension was centrifuged at 800 *g* for 5 min.

NMS873 (Tocris), adarotene/ST1926 (MedChemExpress), XL413 (Selleckchem) were dissolved in dimethyl sulfoxide (DMSO); hydroxyurea (Sigma) was dissolved in water. The treatment of cells was performed for the indicated time at the indicated concentration of inhibitors or an equivalent amount of DMSO. Cell synchronization was carried out by incubating the cells in the presence of 2 mM thymidine (Sigma) for 16 hrs. After that, cells were washed twice with warm PBS and released for the indicated time in drug-free DMEM before the indicated treatments were added.

Whole cell extracts were prepared by adding 50 mM Tris, pH 7.5, 8 M Urea, and 1% Chaps to the cell pellet and vortexing for 30 min at 4ºC, followed by 5 min centrifugation at 20000 *g* and 4ºC. The supernatant was collected as whole cell extract. Subcellular fractionation was carried out as previously described[75]. After the isolation of the cytosolic and nuclear extracts, the chromatin fraction was obtained adding 50 mM Tris, pH 7.5, 8 M Urea, and 1% Chaps to the pellet remaining after nuclear extraction.

Transfection of HCT116 cells with specific siRNA was carried out using Lipofectamine RNAimax (Invitrogen) according to the manufacturer's instructions and using pools of 4 specific siRNA directed against POLA1, POLA2, PRIM1 or PRIM2 (Dharmacon, ON-TARGETplus SMARTPool). As a control cells were transfected with All-stars control (Qiagen). U2OS cells were transfected using DharmaFECT™ following manufacturer's guidelines with a mixture of two siRNA against ETAA1 (UGACAAAGCAGUUAGGUAA[dT][dT] and GAGCAAAACAAGAGGAAUU[dT][dT]) or a single siRNA against TOPBP1 (GGAUAUAUCUUUGCGGUUU[dT][dT]) using the following sequence as negative control (UAACGACGCGACGACGUAAtt).

Antibodies

The antibodies against USP7 (Bethyl A300-033A), VCP (Bethyl A300-589A), SUMO2/3 (MBL, M114-3 and University of Iowa, clone 8A2), PCNA (Santa Cruz, sc-56), Chk1 (Novocastra and Cell Signalling #2360), Chk1-S345P (Cell Signaling #2348), RPA2 (Abcam ab2175), RPA2-S4/S8P (Bethyl, A300-245A), H2A (Cell Signaling #3636), γH2AX (Millipore, 05-636), Ubiquitin (Cell Signaling #3933), MCM2 (custom made, Juan Méndez[76]), MCM2-S40P (Abcam, ab133243), MCM2-S53P (Abcam, ab70367), POLA1 (Abcam, ab31777), PRIM2 (Invitrogen PA5-88189), TOPBP1 (Bethyl, A300-111), Vinculin (Sigma-Aldrich V9264), UFD1L (Abcam, ab155003), CDC25A (Santa Cruz Biotechnology sc-7389) were used for Western Blot and immunofluorescence. VCP (Abcam, ab11433), PRIM2 (Invitrogen PA5-88189) and POLA1 (Abcam, ab31777) antibodies were used for immunoprecipitation.

Flow Cytometry

For the analysis of the cell cycle, cells were incubated with 20 μM EdU for 30 minutes. Then, cells were trypsin-digested, washed with cold PBS once and fixed in 4% PFA/PBS for 15' at room temperature. After permeabilization with 0.25 % Triton/PBS for 20' at room temperature, the EdU was labelled by a Click reaction with a fluorescent azide in the presence of 10 mM Sodium Ascorbate, 2 mM CuSO4 in PBS for 30' at room temperature. Then, the DNA was stained with DAPI 0.5 μg/ml in the presence of 0.25 mg/ml RNAse A. All samples were analyzed in a BD LSRFortessa or in a FACSCanto II cell analyzer. The results were analyzed using the FlowJo software (FlowJo, LLC).

DNA fiber assays

For the analysis of fork rate and origin firing, HCT116 cells were sequentially pulse-labeled with CldU and IdU for 20 min. For the analysis of fork symmetry, HCT116 cells were sequentially pulse-labeled with CldU for 10 min and IdU for 30 min. DNA fibers were spread in buffer containing 0.5% SDS, 200 mM Tris pH 7.4 and 50 mM EDTA. The CldU and IdU tracks were detected by IF with anti BrdU antibodies (rat for CldU, Abcam ab6326, and mouse for IdU, BD 347580). Fiber integrity was assessed with a mouse anti-ssDNA antibody (Millipore MAB3034). Slides were examined with a Leica DM6000 B microscope, as described previously[43]. The conversion factor used was 1 μm=2.59 kb[77]. Signals

were measured and quantified using ImageJ software[78]. For FR, 250-350 forks (red-green tracks) were measured per condition in each independent experiment. For origin firing, origins labeled during the first pulse (green-red-green structures) were quantified as percentage of all structures containing red (>500 total structures scored in each case). For CldU/IdU ratio, red and green labels in 150 ongoing forks were measured. For terminations "only red" signals were quantified as percentage of all structures containing red (>500 total structures scored in each case)[79]. For origin asymmetry, both green tracks coming from a single origin were measured in 50 origins per condition in each independent experiment. An origin is considered asymmetric when the ratio between the two forks (long/short) is greater than 1.4.

Cross-linking with DSP

VCP immunoprecipitation after cross-linking was performed as described in Xue *et al*[38]. After the indicated treatments, cells were incubated in the presence of the cross-linking agent Dithiobis[succinimidyl propionate] (DSP) (Thermo Fisher Scientific, Waltham, MA). DSP stock solution was freshly prepared at 200 mM in DMSO and diluted to 1 mM in PBS. After washing cells twice with PBS and incubating them with DSP for 20 min at room temperature, DSP was replaced with 25 mM Tris-HCl (pH 7.4) to quench the reaction for 10 min at room temperature. Next, cells were scraped in ice-cold PBS and stored at -20°C. The cell pellet was resuspended in buffer A (25 mM Tris-HCl pH 7.4, 150 mM NaCl, 1 mM EDTA, 5% glycerol, 1% Nonidet P-40), lysed by sonication at 4ºC and the lysates were centrifuged at 20,000 *g* for 5 min at 4ºC.

Immunoprecipitation

0.5-1 mg of protein were diluted at 1 mg/ml in BC200 (50 mM Tris pH 7.9, 200 mM NaCl), centrifuged for 5 min at 20,000 *g* at 4 °C and the supernatant collected as input material. After washing protein G Dynabeads (Invitrogen) twice in BC200, the beads were incubated with anti-VCP antibody, anti-PRIM2 antibody or a non-specific IgG in the presence of 0.1 mg/ml BSA in BC200 for 30' at 4ºC. Next, the Dynabeads were washed 5 times in BC200, incubated with the cleared supernatant ON at 4ºC and then washed five times with BC200 with 0.05%

IGEPAL CA630 (Sigma, St. Louis, MO). Bound material was eluted in loading buffer by heating for 10' at 70ºC.

ACKNOWLEDGEMENTS

Research was funded by grants from the Spanish Ministry of Science (BFU2014-55168-JIN; RTI2018-093485-B-I00, co-financed with European FEDER funds) and a Ramón y Cajal Fellowship (RYC-2016-20705) to Emilio Lecona; grant from the Spanish Ministry of Science (PID2019-106707-RB, co-financed with European FEDER funds) to Juan Méndez; and an ERC Starting Grant (ERC-StG-679754) and a grant from the Danish National Research Foundation, Denmark (DNRF115)a (BES-2015-075758) to Luis Toledo.

AUTHOR CONTRIBUTIONS

Sara Rodríguez-Acebes and Rodrigo Martín-Rufo carried out most of the experiments in the study. Alejandro Fernández-Llorente and Guillermo de la Vega-Barranco carried put some experiments in Figures 4 and 5. Pilar Oroz carried out the experiment in Figure S2A. Elena Martín-Doncel carried out the experiment in Figure 3D. Juan Méndez and Luis Toledo contributed to experimental design and the correction of the manuscript. Emilio Lecona designed the experiments, coordinated the study, and wrote the manuscript.

CONFLICT OF INTEREST

The authors declare no conflicts of interest.

REFERENCES

1. Lecona, E. & Fernández-Capetillo, O. Replication stress and cancer: it takes two to tango. *Exp. Cell Res.* **329**, 26–34 (2014).
2. Zeman, M. K. & Cimprich, K. A. Causes and consequences of replication stress. *Nat. Cell Biol.* **16**, 2–9 (2014).
3. Cortez, D. Replication-Coupled DNA Repair. *Mol. Cell* **74**, 866–876 (2019).
4. Lecona, E. & Fernandez-Capetillo, O. Targeting ATR in cancer. *Nat. Rev. Cancer* **18**, 586–595 (2018).
5. Simoneau, A. & Zou, L. An extending ATR-CHK1 circuitry: the replication stress response and beyond. *Curr. Opin. Genet. Dev.* **71**, 92–98 (2021).
6. Daigh, L. H., Liu, C., Chung, M., Cimprich, K. A. & Meyer, T. Stochastic Endogenous Replication Stress Causes ATR-Triggered Fluctuations in CDK2 Activity that Dynamically Adjust Global DNA Synthesis Rates. *Cell Syst.* **7**, 17-27.e3 (2018).
7. Yin, Y. *et al.* A basal-level activity of ATR links replication fork surveillance and stress response. *Mol. Cell* **81**, 4243-4257.e6 (2021).
8. Parker, M. W., Botchan, M. R. & Berger, J. M. Mechanisms and regulation of DNA replication initiation in eukaryotes. *Crit. Rev. Biochem. Mol. Biol.* **52**, 107–144 (2017).
9. Kunkel, T. A. & Burgers, P. M. J. Arranging eukaryotic nuclear DNA polymerases for replication: Specific interactions with accessory proteins arrange Pols α, δ, and ϵ in the replisome for leading-strand and lagging-strand DNA replication. *BioEssays* **39**, (2017).
10. Guilliam, T. A. & Yeeles, J. T. P. An updated perspective on the polymerase division of labor during eukaryotic DNA replication. *Crit. Rev. Biochem. Mol. Biol.* **55**, 469–481 (2020).
11. García-Rodríguez, N., Wong, R. P. & Ulrich, H. D. Functions of Ubiquitin and SUMO in DNA Replication and Replication Stress. *Front. Genet.* **7**, 87 (2016).
12. Martín-Rufo, R., de la Vega-Barranco, G. & Lecona, E. Ubiquitin and SUMO as timers during DNA replication. *Semin. Cell Dev. Biol.* S1084-9521(22)00052–0 (2022) doi:10.1016/j.semcdb.2022.02.013.
13. Moreno, S. P. & Gambus, A. Regulation of Unperturbed DNA Replication by Ubiquitylation. *Genes* **6**, 451–468 (2015).
14. Lopez-Contreras, A. J. *et al.* A proteomic characterization of factors enriched at nascent DNA molecules. *Cell Rep.* **3**, 1105–1116 (2013).
15. Dungrawala, H. *et al.* The Replication Checkpoint Prevents Two Types of Fork Collapse without Regulating Replisome Stability. *Mol. Cell* **59**, 998–1010 (2015).
16. Lecona, E. *et al.* USP7 is a SUMO deubiquitinase essential for DNA replication. *Nat. Struct. Mol. Biol.* **23**, 270–277 (2016).
17. Franz, A. *et al.* USP7 and VCPFAF1 define the SUMO/Ubiquitin landscape at the DNA replication fork. *Cell Rep.* **37**, 109819 (2021).
18. van den Boom, J. & Meyer, H. VCP/p97-Mediated Unfolding as a Principle in Protein Homeostasis and Signaling. *Mol. Cell* **69**, 182–194 (2018).
19. Stach, L. & Freemont, P. S. The AAA+ ATPase p97, a cellular multitool. *Biochem. J.* **474**, 2953–2976 (2017).
20. Franz, A. *et al.* CDC-48/p97 coordinates CDT-1 degradation with GINS chromatin dissociation to ensure faithful DNA replication. *Mol. Cell* **44**, 85–96

(2011).
21. Franz, A. *et al.* Chromatin-associated degradation is defined by UBXN-3/FAF1 to safeguard DNA replication fork progression. *Nat. Commun.* **7**, 10612 (2016).
22. Ramadan, K., Halder, S., Wiseman, K. & Vaz, B. Strategic role of the ubiquitin-dependent segregase p97 (VCP or Cdc48) in DNA replication. *Chromosoma* **126**, 17–32 (2017).
23. Maric, M., Maculins, T., De Piccoli, G. & Labib, K. Cdc48 and a ubiquitin ligase drive disassembly of the CMG helicase at the end of DNA replication. *Science* **346**, 1253596 (2014).
24. Moreno, S. P., Bailey, R., Campion, N., Herron, S. & Gambus, A. Polyubiquitylation drives replisome disassembly at the termination of DNA replication. *Science* **346**, 477–481 (2014).
25. Buchberger, A., Schindelin, H. & Hänzelmann, P. Control of p97 function by cofactor binding. *FEBS Lett.* **589**, 2578–2589 (2015).
26. Bodnar, N. O. & Rapoport, T. A. Molecular Mechanism of Substrate Processing by the Cdc48 ATPase Complex. *Cell* **169**, 722-735.e9 (2017).
27. Twomey, E. C. *et al.* Substrate processing by the Cdc48 ATPase complex is initiated by ubiquitin unfolding. *Science* **365**, eaax1033 (2019).
28. Ji, Z. *et al.* Translocation of polyubiquitinated protein substrates by the hexameric Cdc48 ATPase. *Mol. Cell* **82**, 570-584.e8 (2022).
29. Magnaghi, P. *et al.* Covalent and allosteric inhibitors of the ATPase VCP/p97 induce cancer cell death. *Nat. Chem. Biol.* **9**, 548–556 (2013).
30. González Besteiro, M. A. *et al.* Chk1 loss creates replication barriers that compromise cell survival independently of excess origin firing. *EMBO J.* **38**, e101284 (2019).
31. Rodriguez-Acebes, S., Mourón, S. & Méndez, J. Uncoupling fork speed and origin activity to identify the primary cause of replicative stress phenotypes. *J. Biol. Chem.* **293**, 12855–12861 (2018).
32. Bester, A. C. *et al.* Nucleotide Deficiency Promotes Genomic Instability in Early Stages of Cancer Development. *Cell* **145**, 435–446 (2011).
33. Beck, H. *et al.* Cyclin-Dependent Kinase Suppression by WEE1 Kinase Protects the Genome through Control of Replication Initiation and Nucleotide Consumption. *Mol. Cell. Biol.* **32**, 4226–4236 (2012).
34. Larasati, null & Duncker, B. P. Mechanisms Governing DDK Regulation of the Initiation of DNA Replication. *Genes* **8**, E3 (2016).
35. Abdel-Samad, R. *et al.* Mechanism of action of the atypical retinoid ST1926 in colorectal cancer: DNA damage and DNA polymerase α. *Am. J. Cancer Res.* **8**, 39–55 (2018).
36. Ercilla, A. *et al.* Physiological Tolerance to ssDNA Enables Strand Uncoupling during DNA Replication. *Cell Rep.* **30**, 2416-2429.e7 (2020).
37. Van, C., Yan, S., Michael, W. M., Waga, S. & Cimprich, K. A. Continued primer synthesis at stalled replication forks contributes to checkpoint activation. *J. Cell Biol.* **189**, 233–246 (2010).
38. Xue, L. *et al.* Valosin-containing protein (VCP)-Adaptor Interactions are Exceptionally Dynamic and Subject to Differential Modulation by a VCP Inhibitor. *Mol. Cell. Proteomics* **15**, 2970–2986 (2016).
39. Heidelberger, J. B. *et al.* Proteomic profiling of VCP substrates links VCP to

K6-linked ubiquitylation and c-Myc function. *EMBO Rep.* **19**, e44754 (2018).
40. Huang, E. Y. *et al.* A VCP inhibitor substrate trapping approach (VISTA) enables proteomic profiling of endogenous ERAD substrates. *Mol. Biol. Cell* **29**, 1021–1030 (2018).
41. Michael, W. M., Ott, R., Fanning, E. & Newport, J. Activation of the DNA replication checkpoint through RNA synthesis by primase. *Science* **289**, 2133–2137 (2000).
42. Lupardus, P. J., Byun, T., Yee, M.-C., Hekmat-Nejad, M. & Cimprich, K. A. A requirement for replication in activation of the ATR-dependent DNA damage checkpoint. *Genes Dev.* **16**, 2327–2332 (2002).
43. Mourón, S. *et al.* Repriming of DNA synthesis at stalled replication forks by human PrimPol. *Nat. Struct. Mol. Biol.* **20**, 1383–1389 (2013).
44. Tirman, S., Cybulla, E., Quinet, A., Meroni, A. & Vindigni, A. PRIMPOL ready, set, reprime! *Crit. Rev. Biochem. Mol. Biol.* **56**, 17–30 (2021).
45. González-Acosta, D. *et al.* PrimPol-mediated repriming facilitates replication traverse of DNA interstrand crosslinks. *EMBO J.* **40**, e106355 (2021).
46. Lebrec, V., Poteau, M., Morretton, J.-P. & Gavet, O. Chk1 dynamics in G2 phase upon replication stress predict daughter cell outcome. *Dev. Cell* **57**, 638-653.e5 (2022).
47. Fan, Y. *et al.* LRR1-mediated replisome disassembly promotes DNA replication by recycling replisome components. *J. Cell Biol.* **220**, e202009147 (2021).
48. Crncec, A. & Hochegger, H. Triggering mitosis. *FEBS Lett.* **593**, 2868–2888 (2019).
49. Bastos de Oliveira, F. M. *et al.* Phosphoproteomics reveals distinct modes of Mec1/ATR signaling during DNA replication. *Mol. Cell* **57**, 1124–1132 (2015).
50. Lanz, M. C. *et al.* Separable roles for Mec1/ATR in genome maintenance, DNA replication, and checkpoint signaling. *Genes Dev.* **32**, 822–835 (2018).
51. Syljuåsen, R. G. *et al.* Inhibition of human Chk1 causes increased initiation of DNA replication, phosphorylation of ATR targets, and DNA breakage. *Mol. Cell. Biol.* **25**, 3553–3562 (2005).
52. Maya-Mendoza, A., Petermann, E., Gillespie, D. A. F., Caldecott, K. W. & Jackson, D. A. Chk1 regulates the density of active replication origins during the vertebrate S phase. *EMBO J.* **26**, 2719–2731 (2007).
53. Moiseeva, T. N. *et al.* An ATR and CHK1 kinase signaling mechanism that limits origin firing during unperturbed DNA replication. *Proc. Natl. Acad. Sci.* **116**, 13374–13383 (2019).
54. Moiseeva, T. N. & Bakkenist, C. J. Dormant origin signaling during unperturbed replication. *DNA Repair* **81**, 102655 (2019).
55. Moiseeva, T. *et al.* ATR kinase inhibition induces unscheduled origin firing through a Cdc7-dependent association between GINS and And-1. *Nat. Commun.* **8**, 1392 (2017).
56. Mehta, K. P. M. *et al.* CHK1 phosphorylates PRIMPOL to promote replication stress tolerance. *Sci. Adv.* **8**, eabm0314 (2022).
57. Mirman, Z. *et al.* 53BP1-RIF1-shieldin counteracts DSB resection through CST- and Polα-dependent fill-in. *Nature* **560**, 112–116 (2018).
58. Wu, P., Takai, H. & de Lange, T. Telomeric 3' overhangs derive from resection by Exo1 and Apollo and fill-in by POT1b-associated CST. *Cell* **150**,

39–52 (2012).
59. Kolinjivadi, A. M. *et al.* Smarcal1-Mediated Fork Reversal Triggers Mre11-Dependent Degradation of Nascent DNA in the Absence of Brca2 and Stable Rad51 Nucleofilaments. *Mol. Cell* **67**, 867-881.e7 (2017).
60. Simon, A. C. *et al.* A Ctf4 trimer couples the CMG helicase to DNA polymerase α in the eukaryotic replisome. *Nature* **510**, 293–297 (2014).
61. Baris, Y., Taylor, M. R. G., Aria, V. & Yeeles, J. T. P. Fast and efficient DNA replication with purified human proteins. *Nature* **606**, 204–210 (2022).
62. Porcella, S. Y. *et al.* Separable, Ctf4-mediated recruitment of DNA Polymerase α for initiation of DNA synthesis at replication origins and lagging-strand priming during replication elongation. *PLoS Genet.* **16**, e1008755 (2020).
63. Galarreta, A., Valledor, P., Fernandez-Capetillo, O. & Lecona, E. Coordinating DNA Replication and Mitosis through Ubiquitin/SUMO and CDK1. *Int. J. Mol. Sci.* **22**, 8796 (2021).
64. Deshaies, R. J. Proteotoxic crisis, the ubiquitin-proteasome system, and cancer therapy. *BMC Biol.* **12**, 94 (2014).
65. Huryn, D. M., Kornfilt, D. J. P. & Wipf, P. p97: An Emerging Target for Cancer, Neurodegenerative Diseases, and Viral Infections. *J. Med. Chem.* **63**, 1892–1907 (2020).
66. Krastev, D. B. *et al.* The ubiquitin-dependent ATPase p97 removes cytotoxic trapped PARP1 from chromatin. *Nat. Cell Biol.* **24**, 62–73 (2022).
67. Skrott, Z. *et al.* Disulfiram's anti-cancer activity reflects targeting NPL4, not inhibition of aldehyde dehydrogenase. *Oncogene* **38**, 6711–6722 (2019).
68. Skrott, Z. *et al.* Alcohol-abuse drug disulfiram targets cancer via p97 segregase adaptor NPL4. *Nature* **552**, 194–199 (2017).
69. van den Boom, J. *et al.* VCP/p97 Extracts Sterically Trapped Ku70/80 Rings from DNA in Double-Strand Break Repair. *Mol. Cell* **64**, 189–198 (2016).
70. Kilgas, S. *et al.* p97/VCP inhibition causes excessive MRE11-dependent DNA end resection promoting cell killing after ionizing radiation. *Cell Rep.* **35**, 109153 (2021).
71. Singh, A. N. *et al.* The p97-Ataxin 3 complex regulates homeostasis of the DNA damage response E3 ubiquitin ligase RNF8. *EMBO J.* **38**, e102361 (2019).
72. Lecona, E. & Fernandez-Capetillo, O. A SUMO and ubiquitin code coordinates protein traffic at replication factories. *BioEssays News Rev. Mol. Cell. Dev. Biol.* **38**, 1209–1217 (2016).
73. Xia, Y. The Fate of Two Unstoppable Trains After Arriving Destination: Replisome Disassembly During DNA Replication Termination. *Front. Cell Dev. Biol.* **9**, (2021).
74. Ibarra, A., Schwob, E. & Méndez, J. Excess MCM proteins protect human cells from replicative stress by licensing backup origins of replication. *Proc. Natl. Acad. Sci. U. S. A.* **105**, 8956–8961 (2008).
75. Lecona, E. *et al.* Upregulation of annexin A1 expression by butyrate in human colon adenocarcinoma cells: role of p53, NF-Y, and p38 mitogen-activated protein kinase. *Mol. Cell. Biol.* **28**, 4665–4674 (2008).
76. Ekholm-Reed, S. *et al.* Deregulation of cyclin E in human cells interferes with prereplication complex assembly. *J. Cell Biol.* **165**, 789–800 (2004).

77. Jackson, D. A. & Pombo, A. Replicon clusters are stable units of chromosome structure: evidence that nuclear organization contributes to the efficient activation and propagation of S phase in human cells. *J. Cell Biol.* **140**, 1285–1295 (1998).
78. Schneider, C. A., Rasband, W. S. & Eliceiri, K. W. NIH Image to ImageJ: 25 years of image analysis. *Nat. Methods* **9**, 671–675 (2012).
79. Técher, H. *et al.* Replication dynamics: biases and robustness of DNA fiber analysis. *J. Mol. Biol.* **425**, 4845–4855 (2013).

FIGURE LEGENDS

Figure 1. VCP/p97 is necessary for DNA replication.

(A-B) Flow cytometry analysis of DNA content (DAPI) and DNA replication (EdU) in HCT116 cells synchronized in S phase with a single thymidine block, released for 3 hrs and treated with 2 and 5 μM NMS873 for 3 hrs (A) or with 5 μM NMS873 (VCPi) for 3 or 6 hrs (B). The experiments were repeated twice and one representative experiment is shown. (C-H) Stretched DNA fiber analysis in HCT116 cells synchronized with a single thymidine block, released for 2 hrs and treated for 2 hrs with 10 μM NMS873 (VCPi) or DMSO as a control. (C) Scheme of labeling for fork rate and origin firing measures (1st label origin). Cells were sequentially incubated with CldU and IdU for 20 min. The fork rate (FR) (D) and percentage of origins fired during the first labelling time (1st label origins) (E) were measured and quantified after the different treatments. All the experiments were repeated three times; the pool of the three experiments (fork rate, bars represent the median of the pooled data) or the average (1st label origins, %) is shown. (F) Scheme of labeling for fork asymmetry (CldU/IdU) and origin asymmetry (long/short) measures. Cells were sequentially incubated with CldU for 10 min and IdU for 30 min. The ratio CldU/IdU (CldU/IdU ratio) is shown in (G) and the ratio between the long and the short IdU track arising from the same origin (long/short ration) is shown in (H) (individual data are shown in Figure S1B-C). The experiments were repeated twice and the pool of both experiments is shown. (I) Western blot analysis of whole cell extracts obtained from HCT116 cells synchronized by a single thymidine block, released for 2 hrs and treated with 2 mM hydroxyurea (HU), 10 μM NMS873 (VCPi), a combination of both (HU-VCPi) or DMSO as a control (lane 1, C). The levels of total and phosphorylated Chk1 (S345), total and phosphorylated RPA2 (S4/S8), phosphorylated H2AX (γH2AX), total histone H2A and PCNA were measured with specific antibodies. One of two repetitions is shown.

Figure 2. Distinct effects of VCP/p97 in origin firing and fork progression.

(A-F) Stretched DNA fiber analysis in HCT116 cells synchronized with a single thymidine block, released for 2 hrs and treated for 2 hrs with: 10 μM NMS873

(VCPi), 150 μM nucleosides (dNTP), a combination of both or DMSO as a control (A-B); 10 μM NMS873 (VCPi), 20 μM XL413 (CDC7i), a combination of both (VCPi-CDC7i) or DMSO as a control (C-D); 10 μM NMS873 (VCPi), 0.5 μM adarotene (POLAi), a combination of both (VCPi-POLAi) or DMSO as a control (E-F). Cells were sequentially incubated with CldU and IdU for 20 min. The fork rate (FR) (A, C, E) and percentage of origins fired during the first labelling time (1st label origins) (B, D, F) were measured and quantified after the different treatments. All the experiments were repeated twice and the pool of the two experiments (FR, bars represent the median of the pooled data) or the average (1st label origins) is shown. (G-H) Stretched DNA fiber analysis in HCT116 cells synchronized with a single thymidine block, released for 2 hrs and treated for 2 hrs with: 10 μM NMS873 (VCPi), 0.5 μM adarotene (POLAi), a combination of both or DMSO as a control. Cells were sequentially incubated with CldU for 10 min and IdU for 30 min. The ratio CldU/IdU (CldU/IdU ratio) is shown in (G) and the ratio between the long and the short IdU track arising from the same origin (long/short ratio) is shown in (H) (individual data are shown in Figure S2B-E). The experiments were repeated twice and the pool of both experiments is shown. (I-J) Stretched DNA fiber analysis in HCT116 cells synchronized with a single thymidine block, released for 2 hrs and treated for 2 hrs with 0.5 μM adarotene (POLAi), 20 μM XL413 (CDC7i), a combination of both or DMSO as a control. Cells were sequentially incubated with CldU and IdU for 20 min. The fork rate (FR) (I) and percentage of origins fired during the first labelling time (1st label origins) (J) were measured and quantified after the different treatments. All the experiments were repeated twice and the pool of the two experiments (FR, bars represent the median of the pooled data) or the average (1st label origins) is shown. (K) Western blot analysis of whole cell extracts obtained from HCT116 cells synchronized by a single thymidine block, released for 2 hrs and treated with increasing concentrations of adarotene (0.1, 0.2, 0.5, 1 μM) (POLAi) alone or in combination with 10 μM NMS873 (VCPi). The levels of total and phosphorylated Chk1 (S345), total and phosphorylated RPA2 (S4/S8), phosphorylated H2AX (γH2AX) and total histone H2A were measured with specific antibodies. The experiment was repeated three times and one representative result is shown.

Figure 3. VCP/p97 extracts POLA/PRIM to limit the replication stress response activation upon origin firing.

(A) Western blot analysis of the immunoprecipitation of PRIM2 and VCP/p97 from whole nuclear extracts obtained from HCT116 cells synchronized with a single thymidine block, released for 2 hrs and treated for 3 hrs with 5 μM NMS873 (VCPi), 0.5 μM Adarotene (POLAi) or DMSO as a control (C). 2% of the input material is shown together with the pull-down using a non-specific IgG as a negative control. A saturated exposure is included for VCP/p97 to show the material pulled-down by PRIM2. (B) Western blot analysis of the chromatin fraction purified from HCT116 cells that were synchronized with a single thymidine block, released for 2 hrs and treated for 3 hrs with 5 μM NMS873 (VCPi) or DMSO as a control (marked as C). The levels of POLA1, PRIM2 and VCP/p97 were analyzed with specific antibodies; PCNA and histone H2A were used as controls. (C) Western blot analysis of the chromatin and nuclear soluble fractions purified from HCT116 cells synchronized with a single thymidine block, released for 2 hrs and treated for 2 hrs with 5 μM NMS873 (VCPi), 0.5 μM adarotene (POLAi), 20 μM XL413 (CDC7i), combinations of these drugs or DMSO as a control (marked as C). The levels of POLA1, PRIM2 and total RPA2 were analyzed in chromatin using histone H2A as a control and the levels of total and phosphorylated CHK1 (S345) were analyzed in the nuclear soluble fraction using USP7 as a control. Experiments in (A-C) were repeated at least three times and one representative result is shown. (D) U2OS cells were transfected with a non-specific siRNA or siRNA pools directed against TOPBP1 or ETAA1. 72 hrs after the transfection the cells were treated with 10 μM NMS873 (VCPi), 0.5 μM adarotene (POLAi) or a combination of both using DMSO as a control. Western blot analysis of whole cell extracts with antibodies against TOPBP1, total and phosphorylated CHK1 (S345) using vinculin as a control. The experiment was performed twice with similar results.

Figure 4. VCP/p97 extracts POLA/PRIM to limit the replication stress response activation upon origin firing.

HCT116 cells were transfected with a non-specific siRNA (siC) or with siRNA pools directed against POLA1, POLA2, PRIM1 or PRIM2. 24 hrs after

transfection cells were synchronized with a single thymidine block, released for 2 hrs and treated with 2 or 10 μM NMS873 (VCPi) for 2 hrs or DMSO as control. (A-B) Western blot analysis of whole cell extracts measuring the levels of total and phosphorylated CHK1 (S345), total and phosphorylated RPA2 (S4/S8), phosphorylated H2AX (γH2AX), VCP/p97 and histone H2A and PCNA as controls. The experiments were repeated three times and one representative result is shown. (C-F) Stretched DNA fiber analysis of HCT116 cells depleted in POLA1 or PRIM2. (C-D) Cells were sequentially incubated with CldU and IdU for 20 min. The fork rate (FR) (C) and percentage of origins fired during the first labelling time (1st label origins) (D) were measured and quantified after the different treatments. All the experiments were repeated twice and the pool of the two experiments (FR; bars represent the median of the pooled data) or the average (1st label origins) is shown.

Figure 5. VCP/p97 prevents the activation of the G2/M checkpoint.

(A) Model for the action of VCP/p97 during an unperturbed S phase. POLA/PRIM is loaded to chromatin upon origin firing and generates primed DNA that activates ATR in a TOPBP1 dependent manner. VCP/p97 extracts POLA/PRIM to limit the activation of CHK1. (B) Flow cytometry analysis of the cell cycle progression showing histograms for DNA content by DAPI staining in HCT116 cells arrested with a single thymidine block, released for 3 hrs and treated for 9 hrs with 10 μM NMS873 (VCPi), 2.5 μM LY2603618 (CHK1i), a combination of both (VCPi-CHK1i) or DMSO as a control. (C) Western blot analysis in whole cell extracts in HCT116 cells treated as in (B). The levels of total and phosphorylated CHK1 (S345), total and phosphorylated RPA2 (S4/S8), CDC25A, phosphorylated H2AX (γH2AX), histone H2A and PCNA were measured using specific antibodies. The experiments were repeated twice with equivalent results.

SUPPLEMENTARY FIGURE LEGENDS

Figure S1. Analysis of the effect of VCP/p97 inhibition on DNA replication termination and fork symmetry. Related to Figure 1.

Stretched DNA fiber analysis as in Figure 1C-H. (A) The percentage of terminated forks was quantified showing the mean of two independent experiments. (B-C) Individual measures of the length of the right and left fork arising from a single origin was measured in control conditions (B) and after treatment with VCPi (C) corresponding to Figure 1H. The pool from two experiments is shown. Dotted lines represent a deviation of 40% from the bisectrice of the graph (ideal symmetric forks), as a reference for asymmetry. (D) The percentage of asymmetric origins was quantified showing the mean of two independent experiments.

Figure S2. Regulation of origin firing and fork progression by VCP/p97. Related to Figure 2.

(A) Western blot analysis in whole cell extracts of HCT116 cells treated as in Figure 2C-D. The levels of total and phosphorylated MCM2 (S40 and S53) and PCNA were measured with specific antibodies. The experiment was performed twice with similar results. (B-E) The length of the right and left fork arising from a single origin (from Figure 2H) was measured in control conditions (B) and after treatment with VCPi (C), POLA1 (D) or a combination of both (E). The pool from two experiments is shown. Dotted lines represent a deviation of 40% from the bisectrice of the graph (ideal symmetric forks), as a reference for asymmetry. (F) The percentage of asymmetric origins was quantified showing the mean of two independent experiments. (G) Western blot analysis as in Figure 2K showing that VCPi and POLAi treatment does not change the levels of POLA1, VCP or ubiquitylated proteins.

Figure S3. The control of the replication stress response by VCP/p97 is related to origin firing. Related to Figure 3.

(A) WB analysis of the immunoprecipitation of VCP after cross-linking in HCT116 cells synchronized with a single thymidine block, released for 2 hrs and treated for 3 hrs with DMSO (marked as C), 5 μM NMS873 (VCPi) or 0.5 μM adarotene (POLAi) for 2 hrs. Pull-down with a non-specific IgG was used as control and 2%

of the input material is shown. VCP/p97 and POLA1 were detected using specific antibodies and histone H2A was used as control. One representative experiment out of three repetitions is shown. (B) Western blot analysis of the immunoprecipitation of POLA1 from whole nuclear extracts obtained from HCT116 cells synchronized with a single thymidine block, released for 2 hrs and treated for 3 hrs with 5 μM NMS873 (VCPi), 0.5 μM Adarotene (POLAi) or DMSO as a control (marked as C). 2% of the input material is shown together with the pull-down using a non-specific IgG as a negative control. (C) Flow cytometry analysis of DNA content (DAPI) and DNA replication (EdU) in HCT116 cells wild-type and PRIMPOL knockout synchronized in S phase with a single thymidine block, released for 2 hrs and treated with DMSO (marked as C), 5 μM NMS873 (VCPi), 0.5 μM adarotene (POLAi) or a combination of both (VCPi-POLAi) for 2 hrs. The experiment was repeated twice and one representative experiment is shown. (D) Flow cytometry analysis of DNA content (DAPI) and DNA replication (EdU) in HCT116 cells synchronized in S phase with a single thymidine block, released for 2 hrs and treated with DMSO (marked as C), 5 μM NMS873 (VCPi), 0.5 μM adarotene (POLAi), 20 μM XL413 (CDC7i) or the indicated combinations for 2 hrs. The experiment was repeated three times and one representative experiment is shown. A bar is added as a reference.

Figure S4. Effect of POLA1 and PRIM2 depletion on fork symmetry. Related to Figure 4.

(A-B) Western Blot analysis of the levels of POLA1, PRIM2 and PRIM1 in HCT116 cells transfected with siRNA against POLA1, POLA2, PRIM1 and PRIM2, and treated with DMSO (marked as C) or with 2 or 10 μM NMS873 (VCPi), as in Figure 4A-B. The experiments were repeated three times and the result corresponding to Figure 4A-B is shown. (C-D). Cells were sequentially incubated with CldU for 10 min and IdU for 30 min. The ratio CldU/IdU (CldU/IdU ratio) is shown in (E) and the ratio between the long and the short IdU track arising from the same origin (long/short ratio) is shown in (G). The experiments were repeated twice and the pool of both experiments is shown; bars represent the median of the pooled data. (E-J) Individual measures of the length of the right and left fork arising from a single origin was measured in control depleted cells

(E, control with DMSO and H, treated with VCPi), after depletion of POLA1 (siPOLA1) (F, control with DMSO and I, treated with VCPi) and after depletion of PRIM2 (siPRIM2) (G, control with DMSO and J, treated with VCPi). Dotted lines represent a deviation of 40% from the bisectrice of the graph (ideal symmetric forks), as a reference for asymmetry.

Figure 1

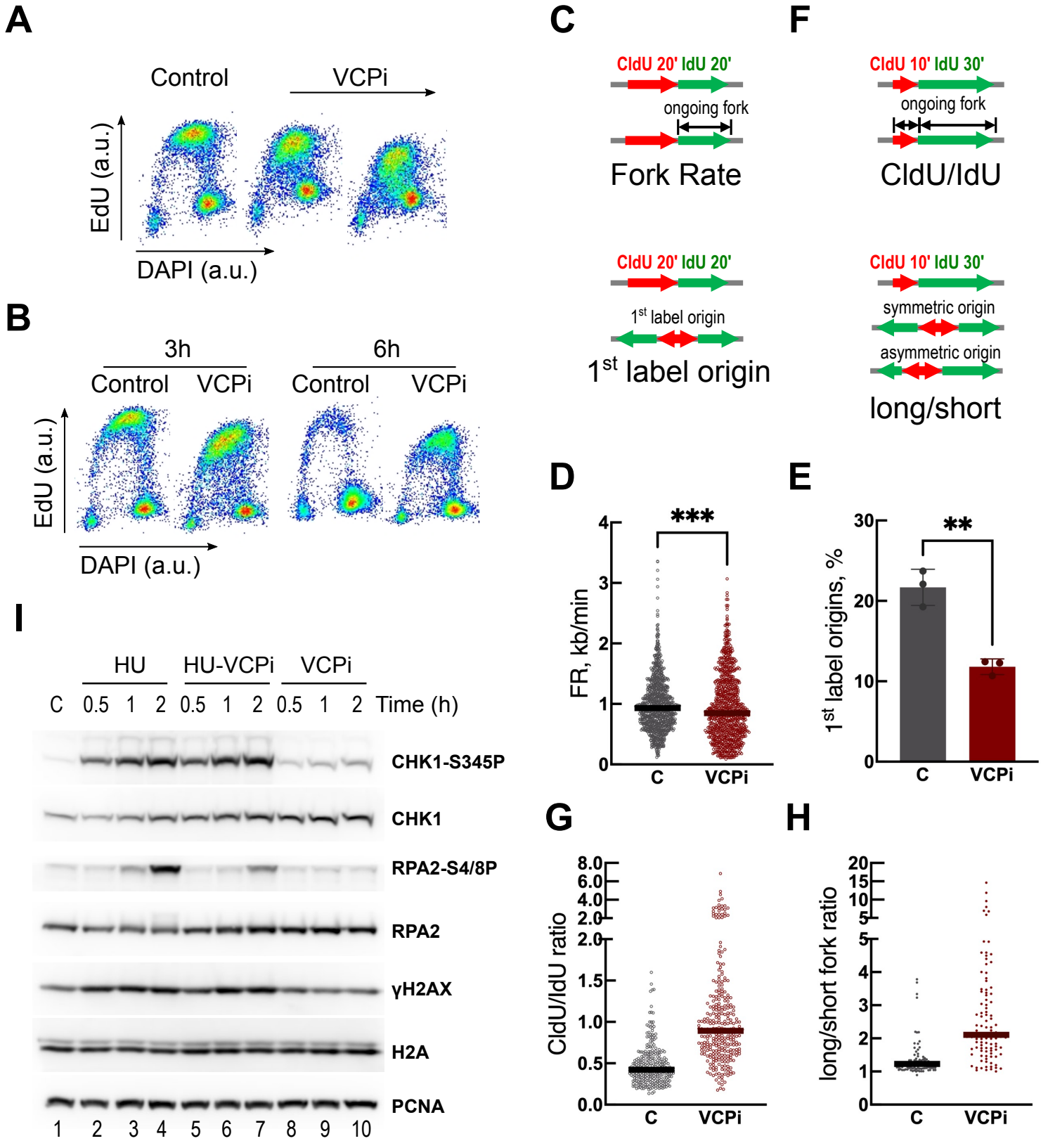
A
Control
VCPi
EdU (a.u.)
DAPI (a.u.)
B
3h
6h
Control
VCPi
Control
VCPi
EdU (a.u.)
DAPI (a.u.)
C
CldU 20' IdU 20'
ongoing fork
Fork Rate
CldU 20' IdU 20'
1st label origin
1st label origin
F
CldU 10' IdU 30'
ongoing fork
CldU/IdU
CldU 10' IdU 30'
symmetric origin
asymmetric origin
long/short
D
***
FR, kb/min
C
VCPi
E
**
1st label origins, %
C
VCPi
I
HU
HU-VCPi
VCPi
C 0.5 1 2 0.5 1 2 0.5 1 2 Time (h)
CHK1-S345P
CHK1
RPA2-S4/8P
RPA2
γH2AX
H2A
PCNA
1 2 3 4 5 6 7 8 9 10
G
CldU/IdU ratio
C
VCPi
H
long/short fork ratio
C
VCPi

Figure 2

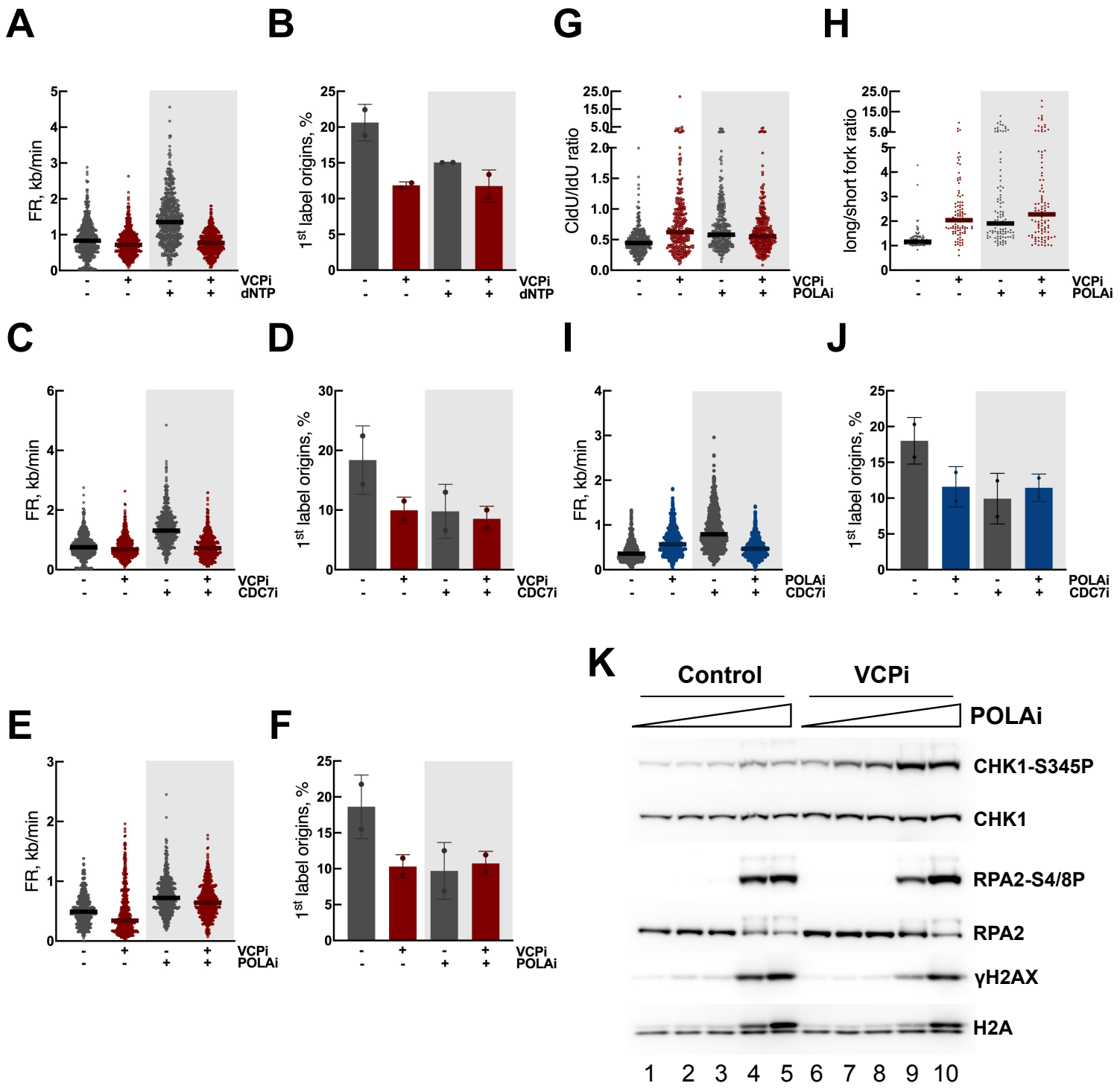
A
FR, kb/min
VCPi
dNTP
B
1st label origins, %
VCPi
dNTP
G
CldU/IdU ratio
VCPi
POLAi
H
long/short fork ratio
VCPi
POLAi
C
FR, kb/min
VCPi
CDC7i
D
1st label origins, %
VCPi
CDC7i
I
FR, kb/min
POLAi
CDC7i
J
1st label origins, %
POLAi
CDC7i
E
FR, kb/min
VCPi
POLAi
F
1st label origins, %
VCPi
POLAi
K
Control
VCPi
POLAi
CHK1-S345P
CHK1
RPA2-S4/8P
RPA2
γH2AX
H2A
1 2 3 4 5 6 7 8 9 10

Figure 3

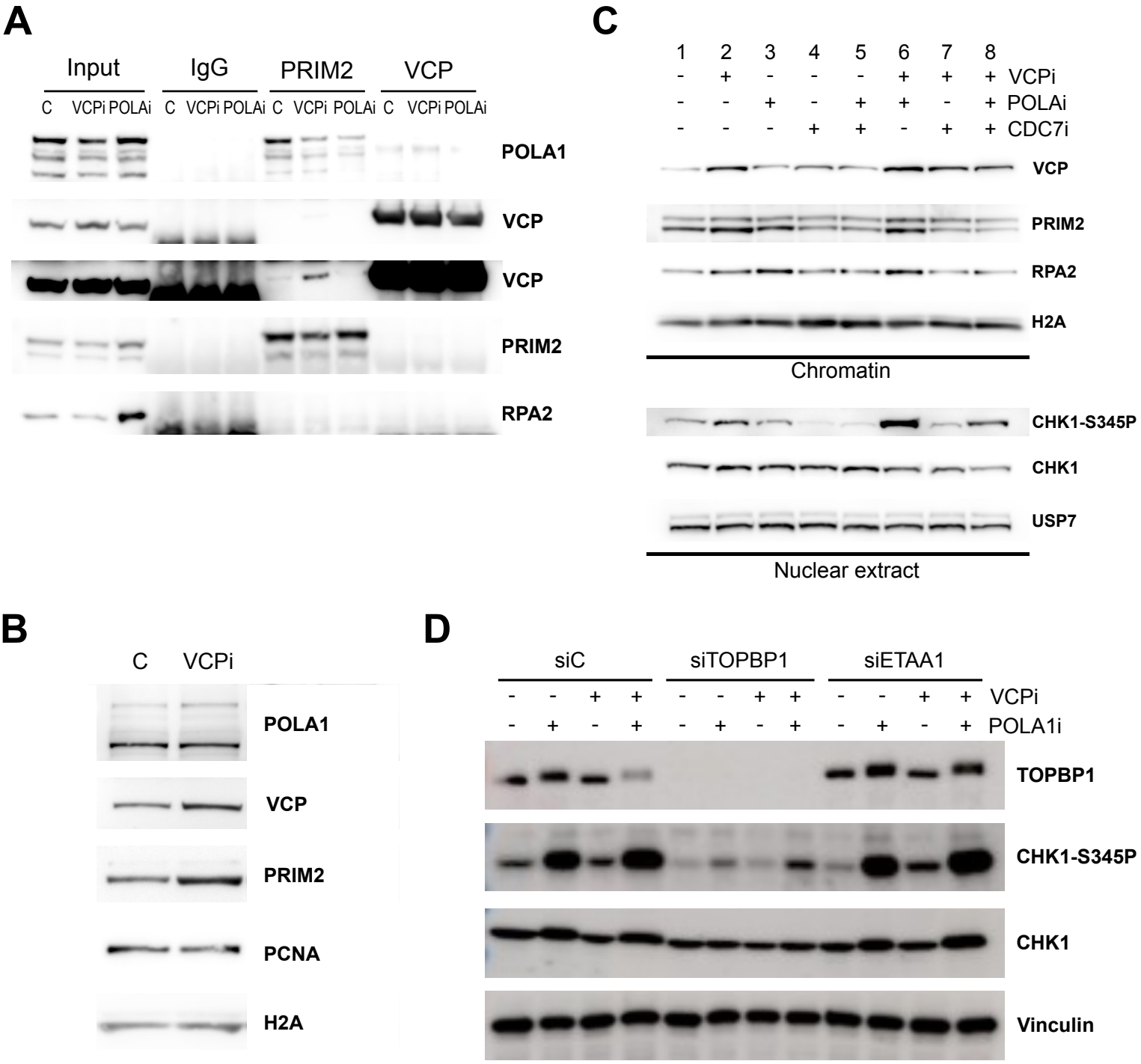
A
Input
IgG
PRIM2
VCP
C VCPi POLAi C VCPi POLAi C VCPi POLAi C VCPi POLAi
POLA1
VCP
VCP
PRIM2
RPA2
C
1 2 3 4 5 6 7 8
- + - - - + + + VCPi
- - + - + + - + POLAi
- - - + + - + + CDC7i
VCP
PRIM2
RPA2
H2A
Chromatin
CHK1-S345P
CHK1
USP7
Nuclear extract
B
C VCPi
POLA1
VCP
PRIM2
PCNA
H2A
D
siC
siTOPBP1
siETAA1
- - + + - - + + - - + + VCPi
- + - + - + - + - + - + POLA1i
TOPBP1
CHK1-S345P
CHK1
Vinculin

Figure 4

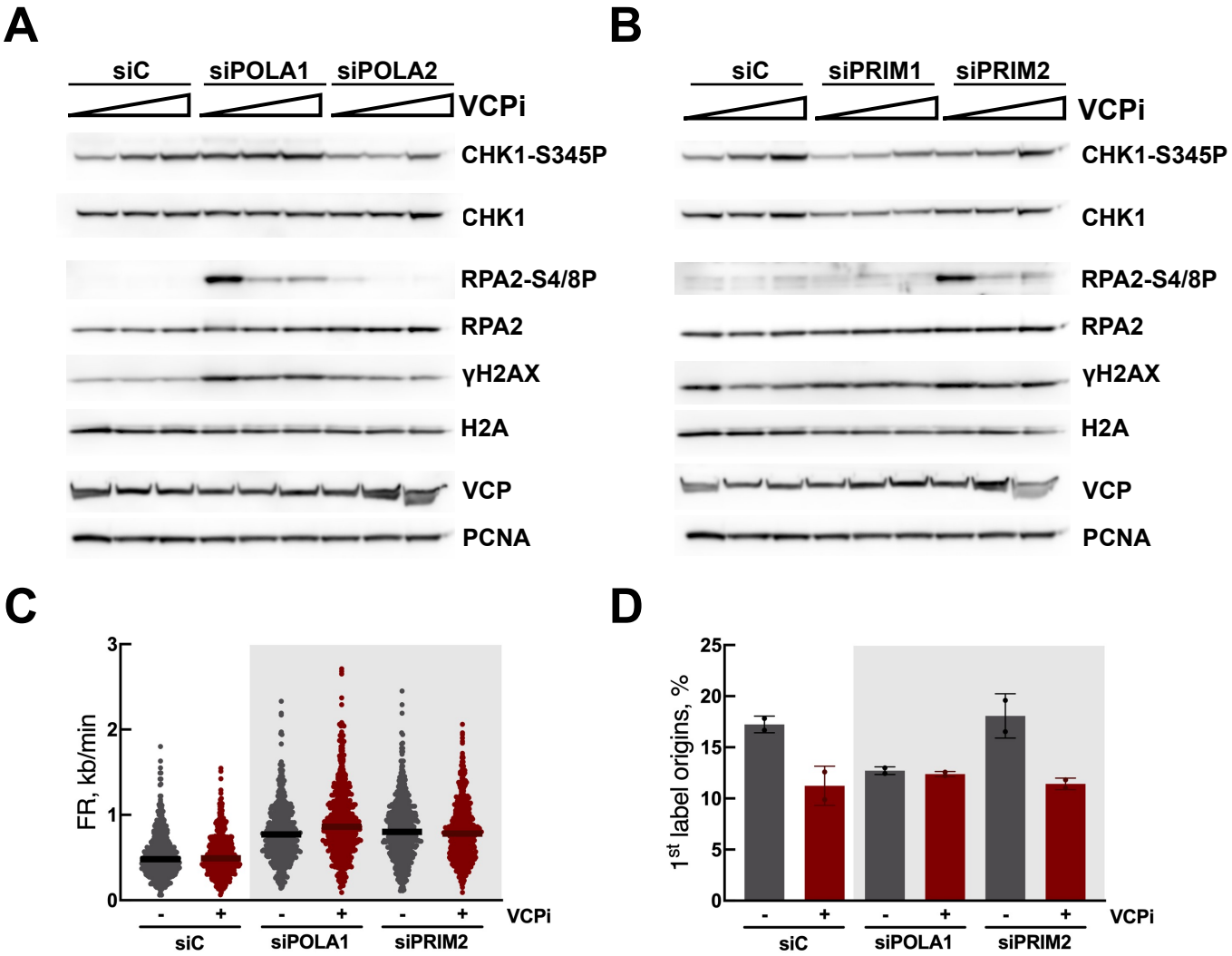
A
siC
siPOLA1
siPOLA2
VCPi
CHK1-S345P
CHK1
RPA2-S4/8P
RPA2
γH2AX
H2A
VCP
PCNA
B
siC
siPRIM1
siPRIM2
VCPi
CHK1-S345P
CHK1
RPA2-S4/8P
RPA2
γH2AX
H2A
VCP
PCNA
C
FR, kb/min
0
1
2
3
-
+
-
+
-
+
VCPi
siC
siPOLA1
siPRIM2
D
1st label origins, %
0
5
10
15
20
25
-
+
-
+
-
+
VCPi
siC
siPOLA1
siPRIM2

Figure 5

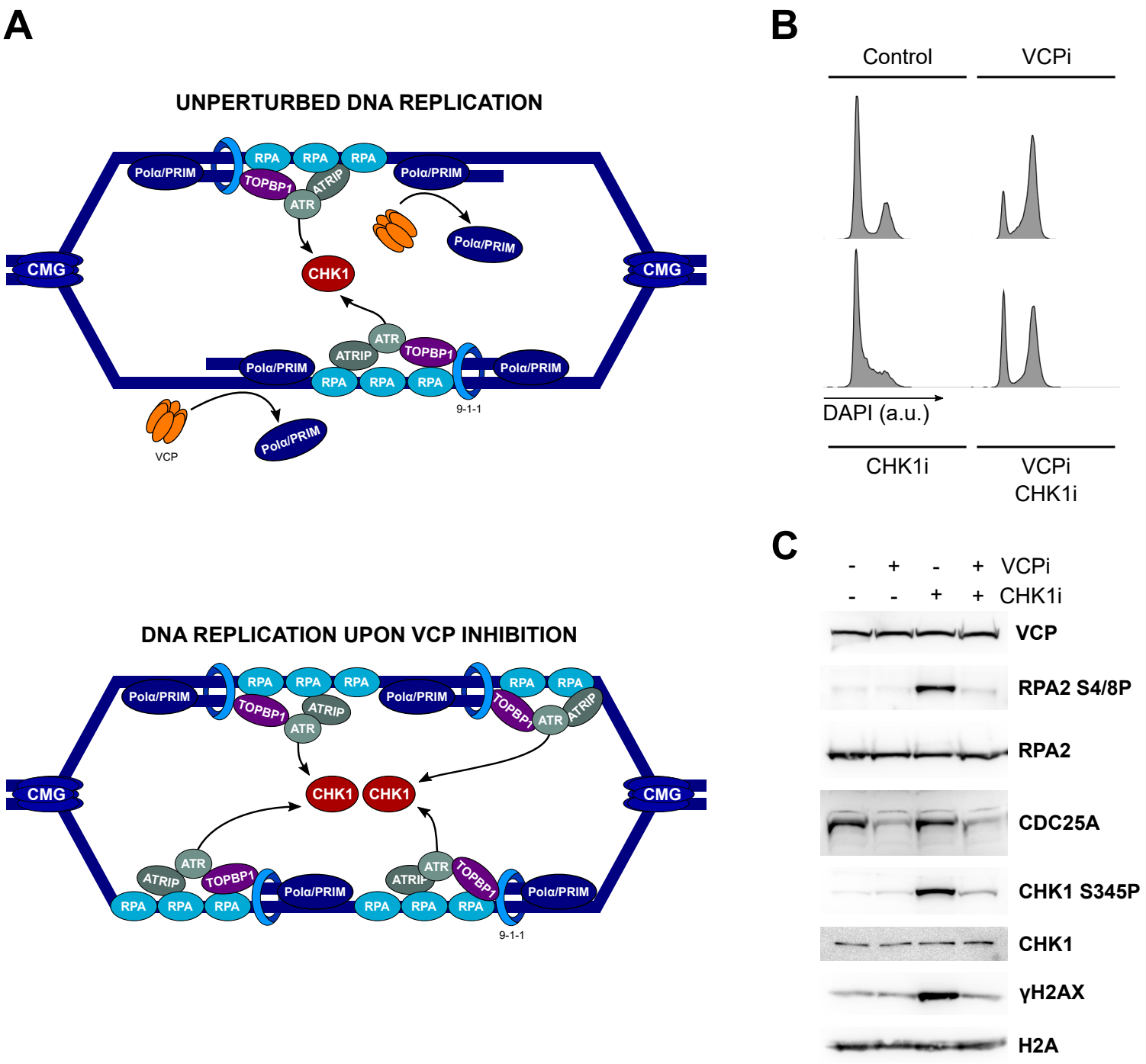
A
UNPERTURBED DNA REPLICATION
Polα/PRIM
RPA
TOPBP1
ATRIP
ATR
CHK1
CMG
VCP
9-1-1
DNA REPLICATION UPON VCP INHIBITION
B
Control
VCPi
DAPI (a.u.)
CHK1i
VCPi
CHK1i
C
- + - + VCPi
- - + + CHK1i
VCP
RPA2 S4/8P
RPA2
CDC25A
CHK1 S345P
CHK1
γH2AX
H2A

Figure S1

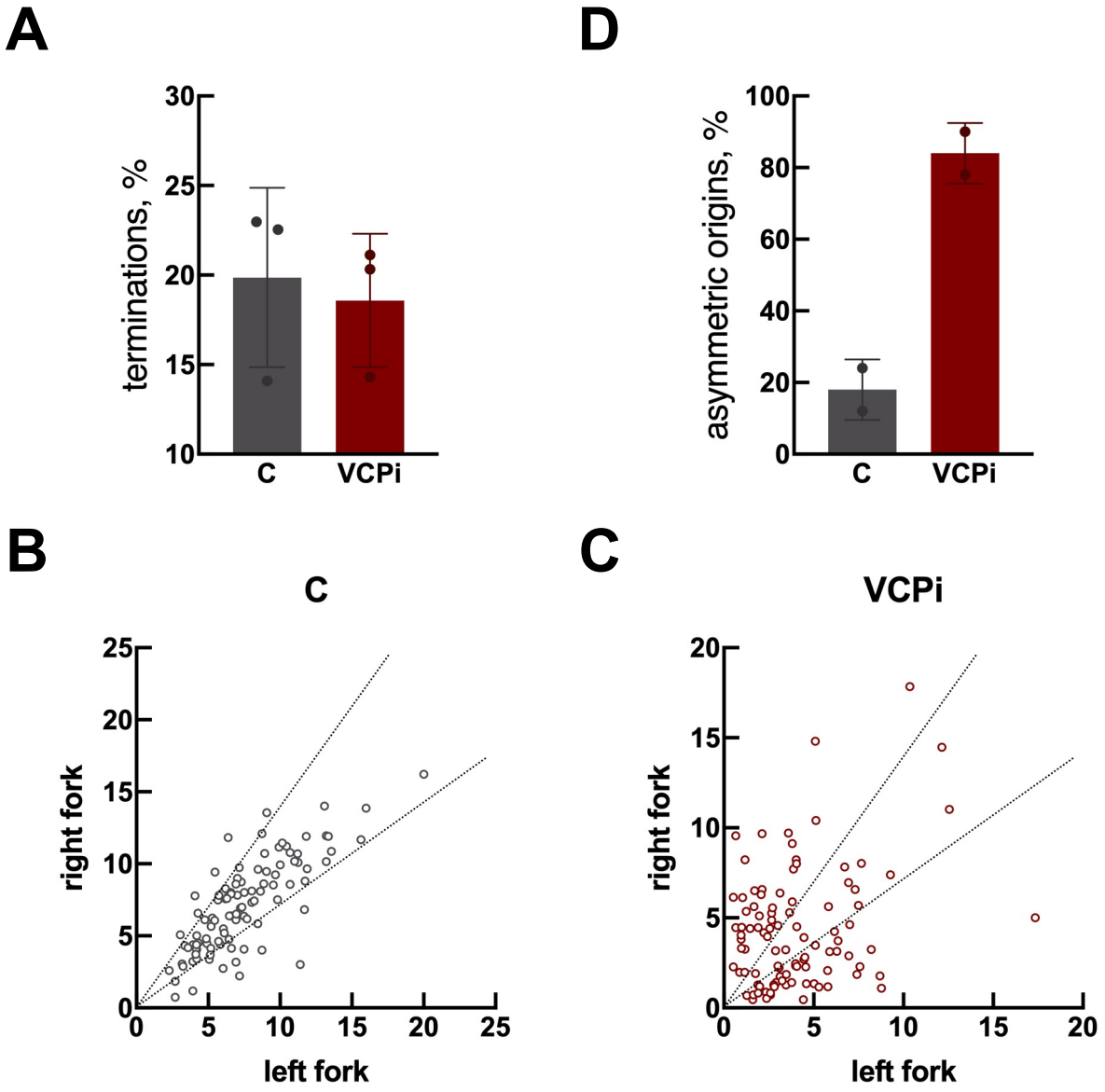
A
terminations, %
30
25
20
15
10
C
VCPi
D
asymmetric origins, %
100
80
60
40
20
0
C
VCPi
B
C
right fork
left fork
0
5
10
15
20
25
C
VCPi
right fork
left fork
0
5
10
15
20

Figure S2

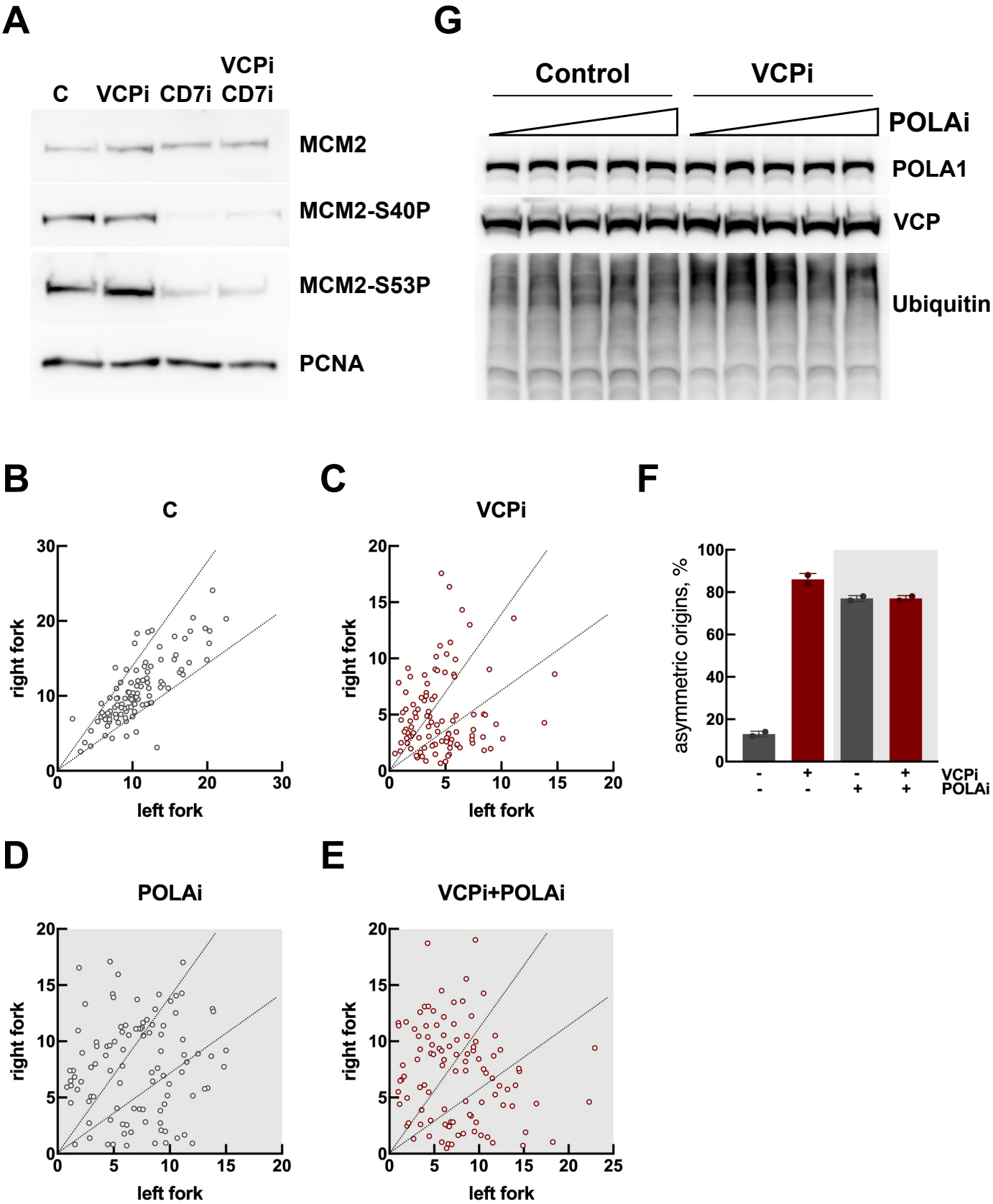
A
C
VCPi
CD7i
VCPi CD7i
MCM2
MCM2-S40P
MCM2-S53P
PCNA
G
Control
VCPi
POLAi
POLA1
VCP
Ubiquitin
B
C
right fork
left fork
D
POLAi
E
VCPi+POLAi
F
asymmetric origins, %
VCPi
POLAi

Figure S3

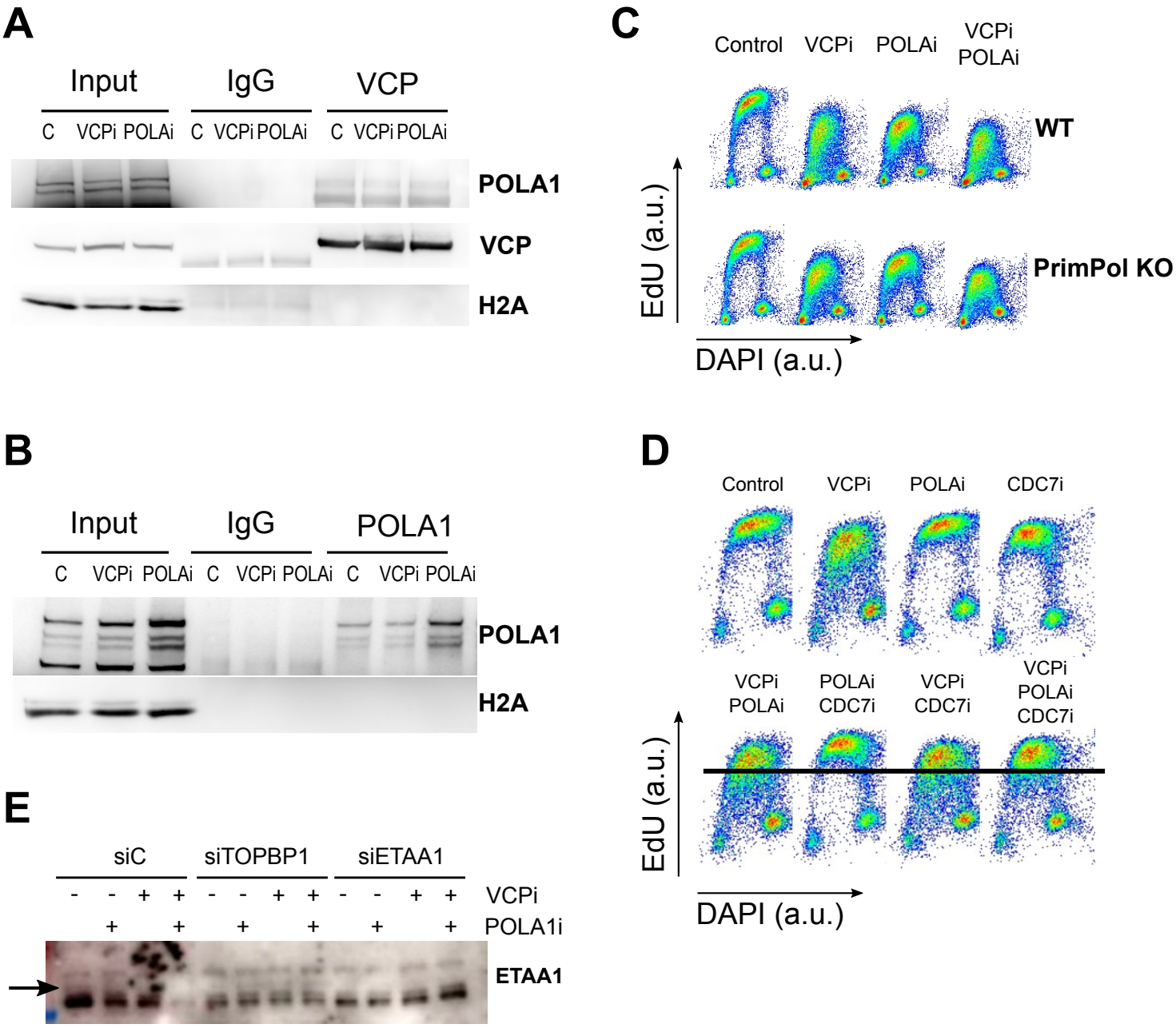
A
Input
IgG
VCP
C VCPi POLAi C VCPi POLAi C VCPi POLAi
POLA1
VCP
H2A
B
Input
IgG
POLA1
C VCPi POLAi C VCPi POLAi C VCPi POLAi
POLA1
H2A
C
Control
VCPi
POLAi
VCPi POLAi
WT
PrimPol KO
EdU (a.u.)
DAPI (a.u.)
D
Control
VCPi
POLAi
CDC7i
VCPi POLAi
POLAi CDC7i
VCPi CDC7i
VCPi POLAi CDC7i
EdU (a.u.)
DAPI (a.u.)
E
siC
siTOPBP1
siETAA1
- - + + - - + + - - + + VCPi
+ + + + + + POLA1i
ETAA1

Figure S4

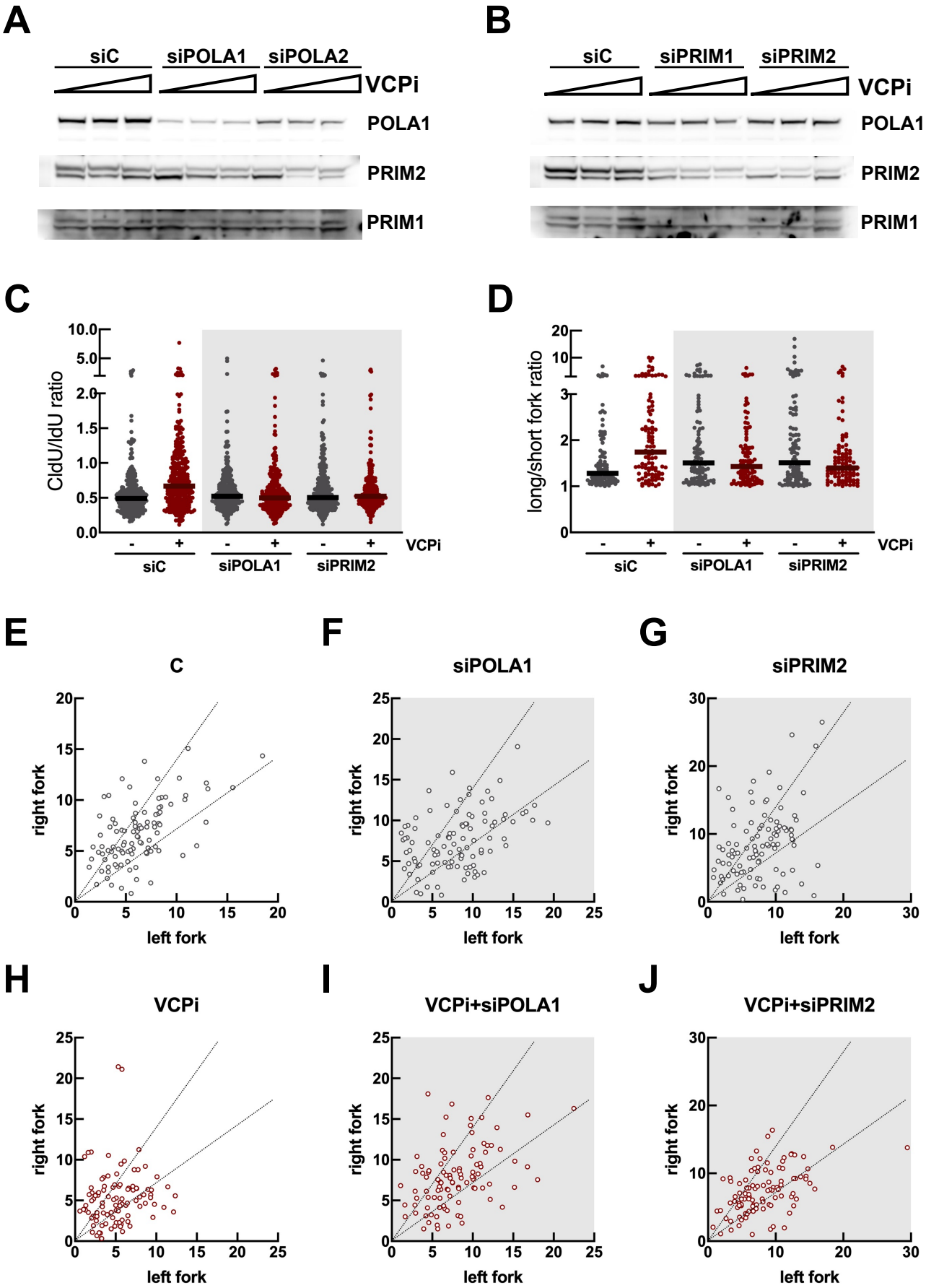
A
siC
siPOLA1
siPOLA2
VCPi
POLA1
PRIM2
PRIM1
B
siC
siPRIM1
siPRIM2
VCPi
POLA1
PRIM2
PRIM1
C
CldU/IdU ratio
10.0
5.0
2.0
1.5
1.0
0.5
0.0
- + - + - +
VCPi
siC
siPOLA1
siPRIM2
D
long/short fork ratio
20
10
3
2
1
0
- + - + - +
VCPi
siC
siPOLA1
siPRIM2
E
C
F
siPOLA1
G
siPRIM2
H
VCPi
I
VCPi+siPOLA1
J
VCPi+siPRIM2
right fork
left fork